

2

DTIC FILE COPY



AFWAL-TR-88-2120

GaAsP TOP SOLAR CELLS FOR INCREASED SOLAR CONVERSION
EFFICIENCY

James B. McNeely
Gerald H. Negley
Allen M. Barnett

ASTROSYSTEMS, INC.
ASTROPOWER DIVISION
30 LOVETT AVENUE
NEWARK, DELAWARE 19711

JANUARY 1989

FINAL REPORT FOR PERIOD JUNE 1985 - SEPTEMBER 1988

Approved for public release; distribution is unlimited.

AERO PROPULSION LABORATORY
AIR FORCE WRIGHT AERONAUTICAL LABORATORIES
AIR FORCE SYSTEMS COMMAND
WRIGHT-PATTERSON AIR FORCE BASE, OHIO 45433-6563

DTIC
ELECTE
14 APR 1989
S E D

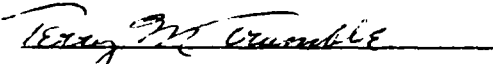
AD-A206 808


NOTICE

WHEN GOVERNMENT DRAWINGS, SPECIFICATIONS, OR OTHER DATA ARE USED FOR ANY PURPOSE OTHER THAN IN CONNECTION WITH A DEFINITELY GOVERNMENT-RELATED PROCUREMENT, THE UNITED STATES GOVERNMENT INCURS NO RESPONSIBILITY OR ANY OBLIGATION WHATSOEVER. THE FACT THAT THE GOVERNMENT MAY HAVE FORMULATED OR IN ANY WAY SUPPLIED THE SAID DRAWINGS, SPECIFICATIONS, OR OTHER DATA, IS NOT TO BE REGARDED BY IMPLICATION, OR OTHERWISE IN ANY MANNER CONSTRUED, AS LICENSING THE HOLDER, OR ANY OTHER PERSON OR CORPORATION; OR AS CONVEYING ANY RIGHTS OR PERMISSION TO MANUFACTURE, USE, OR SELL ANY PATENTED INVENTION THAT MAY IN ANY WAY BE RELATED THERETO.

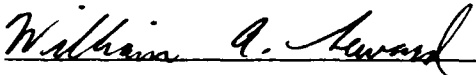
THIS REPORT HAS BEEN REVIEWED BY THE OFFICE OF PUBLIC AFFAIRS (ASD/CPA) AND IS RELEASABLE TO THE NATIONAL TECHNICAL INFORMATION SERVICE (NTIS). AT NTIS, IT WILL BE AVAILABLE TO THE GENERAL PUBLIC, INCLUDING FOREIGN NATIONS.

THIS TECHNICAL REPORT HAS BEEN REVIEWED AND IS APPROVED FOR PUBLICATION.


TERRY M. TRUMBLE
Project Engineer


LOWELL D. MASSIE
Acting Chief, Power Components Branch
Aerospace Power Division

FOR THE COMMANDER


WILLIAM A. SEWARD, Lt Col, USAF
Deputy Director
Aerospace Power Division
Aero Propulsion & Power Laboratory

IF YOUR ADDRESS HAS CHANGED, IF YOU WISH TO BE REMOVED FROM OUR MAILING LIST, OR IF THE ADDRESSEE IS NO LONGER EMPLOYED BY YOUR ORGANIZATION PLEASE NOTIFY AFWAL/POOC, WRIGHT-PATTERSON AFB, OH 45433-6563 TO HELP US MAINTAIN A CURRENT MAILING LIST.

COPIES OF THIS REPORT SHOULD NOT BE RETURNED UNLESS RETURN IS REQUIRED BY SECURITY CONSIDERATIONS, CONTRACTUAL OBLIGATIONS, OR NOTICE ON A SPECIFIC DOCUMENT.

UNCLASSIFIED

SECURITY CLASSIFICATION OF THIS PAGE

REPORT DOCUMENTATION PAGE

1a. REPORT SECURITY CLASSIFICATION UNCLASSIFIED			1b. RESTRICTIVE MARKINGS N/A	
2a. SECURITY CLASSIFICATION AUTHORITY			3. DISTRIBUTION/AVAILABILITY OF REPORT Approved for public release; distribution is unlimited.	
2b. DECLASSIFICATION/DOWNGRADING SCHEDULE N/A				
4. PERFORMING ORGANIZATION REPORT NUMBER(S)			5. MONITORING ORGANIZATION REPORT NUMBER(S) AFWAL-TR-88-2120	
6a. NAME OF PERFORMING ORGANIZATION AstroPower Division Astrosystems, Inc.		6b. OFFICE SYMBOL (If applicable) 8Z012	7a. NAME OF MONITORING ORGANIZATION AeroPropulsion Laboratory (AFWAL/POOC) Air Force Wright Aeronautical Labs.	
6c. ADDRESS (City, State and ZIP Code) 30 Lovell Avenue Newark, DE 19711		7b. ADDRESS (City, State and ZIP Code) Wright-Patterson AFB, OH 45433-6563		
8a. NAME OF FUNDING/SPONSORING ORGANIZATION		8b. OFFICE SYMBOL (If applicable)	9. PROCUREMENT INSTRUMENT IDENTIFICATION NUMBER F33615-86-C-2605	
8c. ADDRESS (City, State and ZIP Code)		10. SOURCE OF FUNDING NOS.		
		PROGRAM ELEMENT NO. 65502F	PROJECT NO. 3005	TASK NO. 20
				WORK UNIT NO. 46
11. TITLE (Include Security Classification) GaAsP Top Solar Cells for Increased Solar Conversion Efficiency				
12. PERSONAL AUTHOR(S) McNeely, James B., Negley, Gerald H., Barnett, Allen M.				
13a. TYPE OF REPORT Final		13b. TIME COVERED FROM 06-85 TO 09-88		14. DATE OF REPORT (Yr., Mo., Day) January 1989
15. PAGE COUNT 49				
16. SUPPLEMENTARY NOTATION This contract was accomplished under the Phase II small business innovative research program.				
17. COSATI CODES			18. SUBJECT TERMS (Continue on reverse if necessary and identify by block number)	
FIELD	GROUP	SUB. GR.		
10	02		Gallium Arsenide Phosphide, Tandem Solar Cells	
09	01		Multijunction Solar Cells, Photovoltaic Devices	
			Solar Energy Conversion Space Power (JES)	
19. ABSTRACT (Continue on reverse if necessary and identify by block number)				
<p>The development of multijunction solar cells is the key to achieving large increases in solar power conversion efficiency over current state-of-the-art technology. In the optimal multijunction design, the <u>top</u> solar cell is the most critical since, by itself, it generates two-thirds of the total power generated by the solar cell stack.</p> <p>There are two viable technical approaches for the top solar cell for the mechanically-stacked tandem solar cell: GaAsP/GaP and AlGaAs/AlGaAs. Both top solar cell approaches have demonstrated good device properties. No other approach has made acceptable devices.</p> <p style="text-align: right;">(See Reverse)</p>				
20. DISTRIBUTION/AVAILABILITY OF ABSTRACT UNCLASSIFIED/UNLIMITED <input checked="" type="checkbox"/> SAME AS RPT <input type="checkbox"/> OTIC USERS			21. ABSTRACT SECURITY CLASSIFICATION UNCLASSIFIED	
22a. NAME OF RESPONSIBLE INDIVIDUAL Terry M. Trumble			22b. TELEPHONE NUMBER (Include Area Code) (513) 255-6235	22c. OFFICE SYMBOL AFWAL/POOC-2

UNCLASSIFIED

SECURITY CLASSIFICATION OF THIS PAGE

Block #19 - Continues

The principal advantage of GaAsP/GaP is in its rugged, transparent mechanical substrate (GaP); the disadvantage of GaAsP lies in the lattice mismatch between the substrate and the active GaAsP device layer.

This contract has been directed to preparing GaAsP/GaP top solar cells with the highest practical transparency and solar cell performance characteristics. The results achieved during this program are in the following table of parameters:

	<u>Target</u>	<u>Actual</u>
Transparency, $< E_g$ (%)	95	95
Voc (volts)	1.46	1.43
Jsc (mA/cm ²)	14.9	14.5 (1.95 eV)
		19.8 (1.78 eV)
FF	0.84	0.84
AM0 Efficiency (%)	13.5	10.6

AstroPower has achieved top solar cell efficiencies of over 10 percent with both GaAsP and AlGaAs materials. To put this in perspective, 13.5 percent is required for 4-terminal, 2-junction efficiency of 25 percent with state-of-the-art silicon bottom solar cells. As a result of this GaAsP program, we have prepared GaAsP solar cells with overall efficiencies of 10.6 percent (AM0). In addition to this, we have recently made lattice-matched AlGaAs top solar cells on 100-micron transparent AlGaAs substrates with 11.2 percent overall conversion efficiency. These results, combined with the greater than 90 percent subbandgap transparency for AlGaAs, are very encouraging.

With indicated improvements in surface recombination for GaAsP and with thick self-supporting AlGaAs, we recommend that a meaningful comparison of the two top solar cell technologies be made to achieve immediate benefits for the Air Force in terms of overall conversion efficiency, array size, survivability, and manufacturability.

Accession For	
NTIS GRA&I	<input checked="" type="checkbox"/>
DTIC TAB	<input type="checkbox"/>
Unannounced	<input type="checkbox"/>
Justification	
By	
Distribution/	
Availability Codes	
Dist	Avail and/or Special
A-1	

UNCLASSIFIED

SECURITY CLASSIFICATION OF THIS PAGE

SUMMARY

The development of multijunction solar cells is the key to achieving large increases in solar power conversion efficiency over current state-of-the-art technology. In the optimal multijunction design, the top solar cell is the most critical since, by itself, it generates two-thirds of the total power generated by the solar cell stack.

There are two viable technical approaches for the top solar cell for the mechanically-stacked tandem solar cell: GaAsP/GaP and AlGaAs/AlGaAs. Both top solar cell approaches have demonstrated good device properties. No other approach has made acceptable devices.

The principal advantage of GaAsP/GaP is in its rugged, transparent mechanical substrate (GaP); the disadvantage of GaAsP lies in the lattice mismatch between the substrate and the active GaAsP device layer. The lattice mismatch makes it harder to passivate the GaAsP emitter surface.

The advantage of AlGaAs is that it is lattice-matched to its substrate. Another advantage is that a range of lattice-matched AlGaAs compositions exists which makes passivation for reduced surface recombination easier. The disadvantage is that the GaAs substrates normally used for epitaxial growth of the AlGaAs are not transparent to the top solar cell subbandgap photons. This substrate must be removed by some means before assembly of the tandem device. This leads to the biggest problem: growth of a thick, mechanically-stable, transparent AlGaAs substrate.

The issue is which of these materials -- GaAsP or AlGaAs -- will result in better top solar cell performance when compared under equivalent conditions. Each material needs to be compared using fabrication techniques that optimize transparency, open-circuit voltage, short-circuit current, fill-factor, and overall conversion efficiency in a systematic way.

The work done during this contract has been directed to preparing GaAsP/GaP top solar cells with the highest practical transparency and solar cell performance characteristics. The results achieved during this program are in the following table of parameters:

	<u>Target</u>	<u>Actual</u>
Transparency, < E_g (%)	95	95
Voc (volts)	1.46	1.43
Jsc (mA/cm^2)	14.9	14.5 (1.95 eV) 19.8 (1.78 eV)
FF	0.84	0.84
AMO Efficiency (%)	13.5	10.6

Present Top Solar Cell Status:

Top Solar Cell Transparency -- This parameter affects the amount of solar photons which will reach the underlying solar cell(s). It is important to the tandem cell overall conversion efficiency that the top solar cell be completely transparent to photons less energetic than the bandgap of the top cell. AstroPower has achieved greater than 95 percent transparency on GaAsP top solar cell structures during this contract.

The key to practical AlGaAs top solar cells lies in maintaining a high degree of transparency while preparing thick (approximately 100 micron thickness) AlGaAs layers. This will eliminate the problems caused by the thin, very fragile AlGaAs layers. In recent work in our laboratories, 91 percent subbandgap transmission was achieved on a self-supporting 120-micron AlGaAs structure. The design of an improved AR coating will lead to transparencies of greater than 96 percent. Furthermore, there has been a recent breakthrough in light-emitting diode efficiency, achieving an external quantum efficiency of 8.0 percent, and resulting in LED's which are over 10 times brighter than earlier devices. These LED's were prepared by liquid-phase epitaxial growth of thick free-standing AlGaAs structures. This same technology of rugged, transparent self-supporting AlGaAs layers can be applied to practical top solar cells.

Open-Circuit Voltage -- Both GaAsP and AlGaAs top solar cells have been prepared in our laboratory with Voc's of 1.3 to 1.55 volts. In recent preliminary work here on AlGaAs, Voc of greater than 1.30 volts was achieved after a short period of time and effort. Further improvements in Voc may be expected from improved p/n junction uniformity and from reduced device dark current.

Short-Circuit Current -- Lattice-mismatched cap layers (e.g., GaP on the top active GaAsP layer) were explored during this contract. Cap layers must be close to lattice-matched so that nucleation of the grown layer is not inhibited locally. Stress/strain from cap layer lattice mismatch must be isolated from the thin emitter layer and junction. These two basic problems have led to the recommendation that future work should be done on lattice-matched cap layers and other chemical surface passivation techniques.

The design and practical attainment of III-V solar cells with near-theoretical Jsc values have required an effective surface passivation to minimize high surface recombination velocities (S_R). With GaAs and lattice-matched AlGaAs, this has been accomplished, in state-of-the-art solar cells, by the use of a higher bandgap heteroface. The high surface recombination

velocities for the non-passivated GaAs surface result from "pinning" of the Fermi level and are now attributed to elemental arsenic or arsenic ions at the semiconductor surface which occur as products of the reaction between the III-V surface and air. Elimination of this arsenic has considerable potential for reduction of S_R in these materials, and appears especially attractive for GaAsP devices at this time.

Surface recombination may be reduced by orders of magnitude by "unpinning" the Fermi level at the emitter surface. "Unpinning" is expected to result in sizeable increases in current collection and reduced dark current (leading to higher Voc) for the GaAsP top solar cells. Arsenic ions on the GaAs (or GaAsP) surface appear to be responsible for high surface recombination in devices made from that material. Inorganic sulfide films have been used on GaAs to reduce surface recombination rates to that of the nearly ideal AlGaAs/GaAs interface.

It is clear, at the present time, that surface recombination is the major limitation to J_{sc} in GaAsP p/n junction top solar cells. The Fermi-level pinning mechanism involving metallic arsenic or arsenic ions at the semiconductor surface applies to GaAsP for the same reason it applies to GaAs. Therefore, there is a well-defined need to establish a suitable nearly-lattice-matched cap layer or surface passivation film, eliminating the arsenic, and any other Fermi pinning mechanism, for GaAsP p-n junction top solar cell devices. This will lead to nearly ideal J_{sc} values and lower dark currents in the top solar cells. Our expectations are that J_{sc} will exceed the 14.9 mA/cm^2 required for a 25 percent tandem stack with the use of a surface passivation layer on GaAsP. The primary problem is finding a lattice-matched or another non-stress inducing layer.

Fill Factor -- Good fill factors have been demonstrated in both the AlGaAs and GaAsP solar cells.

Efficiency -- AstroPower has achieved top solar cell efficiencies of over 10 percent with both GaAsP and AlGaAs materials. To put this in perspective, 13.5 percent is required for 4-terminal, 2-junction efficiency of 25 percent with state-of-the-art silicon bottom solar cells. As a result of the GaAsP program, we have prepared GaAsP solar cells with overall efficiencies of 10.6 percent (AMO). In addition to this, we have recently made lattice-matched AlGaAs top solar cells with 11.2 percent overall conversion efficiency. These results, combined with the greater than 90 percent subbandgap transparency for AlGaAs, are very encouraging.

The present day technology for "unpinning" the Fermi level, as a means of surface passivation, is in its early stages of devel-

opment. Unpinning effects currently are transient and short term laboratory demonstrations. The current technology is sufficient for a fair comparison of the relative GaAsP and AlGaAs performance potential. Then, if GaAsP is determined to be the material of choice, the problem is quite clear for GaAsP top solar cell development:

- o Develop the growth and fabrication of a nearly lattice matched window layer that meets the requirements indicated in 2.1.3.3 of this report; or
- o Develop a long-term, space-qualified surface "unpinning" passivation treatment.

With improved S_p for GaAsP and thick self-supporting AlGaAs, we recommend that a meaningful comparison of the two top solar cell technologies be made to achieve immediate benefits for the Air Force in terms of overall conversion efficiency, array size, survivability, and manufacturability.

In summary, the present opportunity for comparing AlGaAs and GaAsP top solar cell technologies on a quantitative basis in the same laboratory is very attractive. Our recommendations for taking advantage of this opportunity will compare self-supporting (approximately 100 microns thick) AlGaAs top solar cells and surface-passivated GaAsP (on transparent GaP) top solar cells. This work is expected to establish which top solar cell material will exhibit the most promise for 25 percent to 35 percent tandem solar cells.

Accomplishments:

- o First tandem GaAsP on silicon solar cell was demonstrated in July 1986.
- o All four solar cell parameter goals (open-circuit voltage, short-circuit current, fill factor, and top cell transparency) required to demonstrate a 25 percent tandem solar cell have been met individually.
- o Best GaAsP top solar cell results to date:

$\frac{V_{oc}}{(\text{volts})}$	$\frac{J_{sc}}{(\text{mA/cm}^2)}$	$\frac{FF}{(\%)}$	$\frac{Eff.}{(\%)}$
0.901	19.8	0.8	10.6

- o Jsc vs E_g results for the range of GaAsP compositions are 60-80 percent quantum efficiency for the entire range.
- o Two-terminal and four-terminal configurations tandem solar cells are feasible depending on the application.

- o Active layer dislocation levels were reduced by multi-layer grading, minimizing lattice mismatch, and by bismuth grading and/or growth-interrupts.
- o Began window layer development to reduce surface recombination.
- o Device area was increased from 0.1 to 1.0 to 4.0 sq. cm.
- o A 35 percent 3-stack six-terminal tandem cell with GaAsP/GaAs (or InP)/GaInAsP has been conceived.
- o Observed shift in GaP bandedge with nitrogen doping, and attempted to increase photon absorption in indirect GaP material.

TABLE OF CONTENTS

	<u>Page</u>
1. INTRODUCTION	1
2. MAIN TEXT	6
2.1 Description and Discussion of Research Work	6
2.1.1 Tandem Cell Design	6
2.1.2 Growth Technique	8
2.1.3 Solar Cell Device Issues	14
2.1.3.1. Transparency	16
2.1.3.2. Voltage	16
2.1.3.3. Current	19
2.1.3.4. High Performance Design	24
2.1.4 Solar Cell Testing and Characterization Results	27
2.2 Results Achieved	30
3. CONCLUSIONS	30
4. PERSPECTIVE AND RECOMMENDATIONS	31
5. REFERENCES	35

LIST OF FIGURES

<u>Figure</u>		<u>Page</u>
1	Single Junction Solar Cell Efficiencies for Standard Solar Spectra as a Function of Single Junction Bandgap	3
2	Quantum Efficiency of GaAsP and Silicon in a Tandem Cell as a Function of Wavelength	3
3	Theoretical Isoefficiency Curves as a Function of Top and Bottom Solar Cell Bandgaps, for AMO Four-Terminal Operation	4
4	Theoretical Isoefficiency Curves as a Function of Top and Bottom Solar Cell Bandgaps, for AMO Two-Terminal Operation	5
5	Slider Boat Growth Apparatus showing the Graded Well Width	10
6	GaAsP on GaP Top Solar Cell Structure Schematic Drawing	10
7	Compositional Profile of an Edge Cleave of a Bismuth-graded GaP to GaAs LPE Layer Growth	13
8	Improvements in Voltage during this Contract	19
9	Optical Absorption Spectra of Gallium Phosphide with and without Deliberate Nitrogen Doping	22
10	Short-Circuit Current for MIS Devices as a Function of GaAsP Bandgap	24
11	High Performance GaAsP Top Solar Cell	25
12	Quantum Efficiency of GaAsP (and AlGaAs) Top Solar Cells, Compared to Conventional GaAs Space Solar Cell	28
13	GaAsP/Silicon Mechanically-Stacked, Four-Terminal Tandem Solar Cell, 4.0 cm ² Area	29
14	GaAs Surface Band Structure -- "Pinned" and "Unpinned" Surfaces	34

LIST OF TABLES

<u>Table</u>		<u>Page</u>
1	Modelled Theoretical Maximum for Silicon Space Solar Cells Compared to Actual Silicon Results	7
2	Expectation of Best Case GaAsP at 1.97 eV	7
3	Best Case Tandem Solar Cell with Various Silicon Bottom Solar Cells (AM0)	8
4	Comparison of Best Case GaAsP to Requirements for a 25 percent Efficient Four-Terminal Tandem Solar Cell	8
5	Predicted Open-Circuit Voltage for GaAs on GaP with Variable Gratings and Defect Structure	12
6	Anodic Thinning of GaAsP Samples	21
7	Best GaAsP on GaP Solar Cell Parameters	28
8	Top GaAsP Solar Cell Progress	29

1. INTRODUCTION

1.1 Background

1.1.1 Overall benefits of technology

Mechanically-stacked tandem solar cells present the opportunity for major improvement in power density for arrays. Two-junction tandem solar cells can be wired in two-, three-, and four-terminal configurations. The four-terminal tandem solar cell has one major advantage over the multibandgap two-terminal solar cell, the fact that current-matching does not have to be achieved within the tandem stack. A four lead connection to a two solar cell stack allows each solar cell to be connected in a series arrangement to other solar cells of the same type. In a radiation orbit, where radiation to the top and bottom solar cells will cause different degrees of damage, current-matched multibandgap solar cells will operate only as well as the least efficient solar cell in the stack. This current mismatch can result in a significant power loss over the lifetime of the solar array.

The major advantage of tandem GaAsP/Si solar cells over planar single-junction solar cells is in energy conversion efficiency. Using existing technology, planar silicon solar cells usually provide efficiencies of 13 percent to 16 percent. In the near term the tandem GaAsP/Si stack is expected to provide almost 25 percent efficiency. Thus, a one square meter array which formerly produced 160 watts will now produce 297 watts. Although the tandem solar cell is about twice as heavy as a silicon cell, it is approaching almost twice the output. A 10-kilowatt GaAsP/Si array would require only 33.6 square meters of array area as compared to 62.5 square meters for a silicon array. Larger array sizes require more propellants for station keeping and pointing and thus would significantly shorten the useful life of a satellite.

In the optimal multijunction design, the top solar cell performance is the most critical since, by itself, it generates two-thirds of the total power generated by the solar cell stack. Therefore, the development of a 25 percent efficient tandem solar cell is dependent on the development of the top solar cell of the GaAsP/Si stack. The top solar cell must have a transmission of about 60 percent (subbandgap transparency of over 95 percent) and an efficiency of 13.5 percent to provide a tandem stack with 25 percent efficiency. The development of GaAsP top solar cells for mechanical attachment to silicon bottom solar cells can lead to AM0 conversion efficiency increases of 49 percent to 86 percent over the best state-of-the-art single junction solar cells.

There are additional advantages to this tandem structure: the improved radiation resistance of the tandem structure. The bottom silicon cell, which is more prone to radiation damage, is covered and protected by the GaAsP top cell. There is mounting

evidence that wider bandgap materials are correspondingly more radiation resistant. Curtis [1] comparing wide and narrow bandgap materials found that AlGaAs and GaAs were much more radiation resistant than silicon or InGaAs. At the same time, Hamaker et al [2] demonstrated less radiation damage in 1.93 eV AlGaAs solar cells than GaAs counterparts. In very recent results on AstroPower GaP (Bandgap -- 2.26 eV) solar cells, little degradation has been observed by Sandia after the equivalence of ten years' radiation exposure [3]. These GaP devices are the most radiation-hard devices that this particular laboratory at Sandia has observed. For these reasons, we expect the tandem cell to have good stability and reliability during actual radiation exposure conditions in the space environment.

The technical risks associated with the development of a practical tandem solar cell system are minimized because the development is based on reliable state-of-the-art silicon solar cell device and array technology and on compound semiconductor technology which has also matured, reaching a high level of technical sophistication.

The fabrication of GaP and GaAsP solar cells directly benefits from the manufacturing methods technology developed in the last 18 years during the growth and maturing of the lightemitting diode industry. In the period 1970-76, light-emitting diodes became the display technology of choice for electronic designers of calculators, digital watches, and instruments. This technology was based on advances in the manufacturability of GaAsP and GaP materials that resulted from manufacturing methods technology investments by the Air Force and the opto-electronic industry. During this period, fabrication costs for the LED wafers were reduced from \$700-900 per square inch of material to less than \$25 per square inch, and typical fabrication throughputs rose to 80K-150K square inches of GaAsP per month in one of the larger manufacturing facilities producing high-efficiency red light-emitting diodes. These fabrication advantages make it probable that GaAsP top solar cells will be lower cost than alternative materials, and the technical risks in developing the tandem solar cell using this system can be minimized.

1.1.2 Design of tandem cell

Tandem solar cells are more efficient than single junction cells because they operate on the portion of the solar spectrum that matches the characteristic bandgap of the semiconductor material in the tandem cell. Solar cells convert incident solar photons equal to or more energetic than their characteristic bandgap; however, the actual energy difference between the solar photon energy and the characteristic bandgap is wasted and ends up in the form of thermal energy. Incident photons with less energy than the characteristic band gap of the material pass through the material and are unaffected if the material is transparent to the low energy

photons. Fifty-four percent of the energy incident in a single junction silicon cell is wasted by these two mechanisms [4]. Figure 1 illustrates the peak efficiencies that are possible with single-junction material, as a function of bandgap. Multiple junction stacks of semiconductor materials having characteristic bandgaps spaced throughout the solar spectrum can lead to more efficient solar energy conversion than single junction solar cells. To demonstrate the spectral splitting, quantum efficiencies of the two complementary materials (GaAsP, Silicon) are shown in Figure 2.

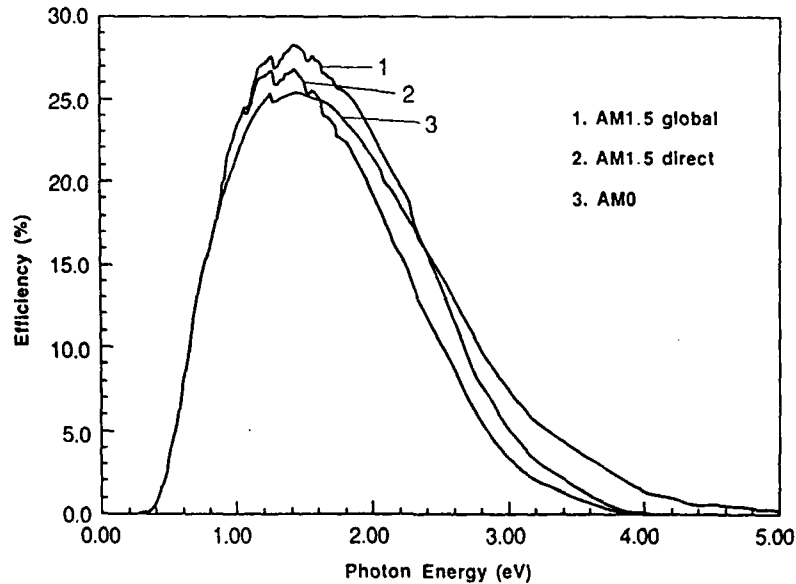


Figure 1. Single Junctions Solar Cell Efficiencies for Standard Solar Spectra as a Function of Single Junction Bandgap.

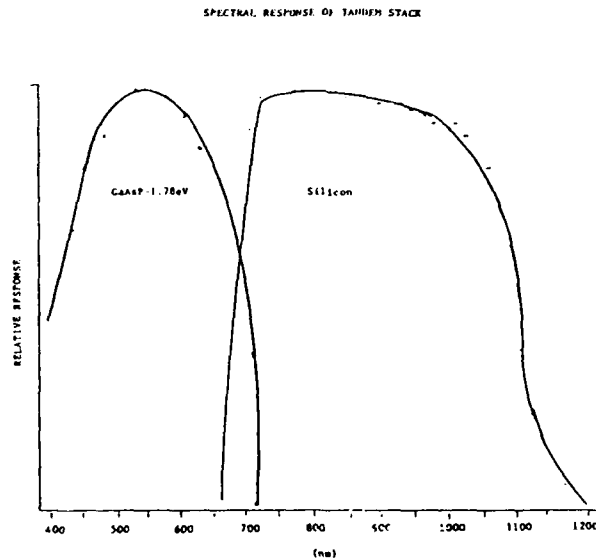


Figure 2. Quantum Efficiency of GaAsP and Silicon in a Tandem Cell as a Function of Wavelength.

The design of tandem solar cells, and, in particular, the mechanically-stacked GaAsP on GaP top solar cell (on a silicon bottom solar cell) is based on a model used to calculate theoretical maximum efficiencies of tandem solar cell systems. The model that is being used is by Nell [5], and refined by Barnett and Terranova [6], and is based upon tabulated standard spectra and fundamental material parameters, and assumes unity quantum efficiency. Using this approach, the open-circuit voltages predicted by the model agree very well with experimental results of well-developed solar cells.

Using solar irradiance information, the performance is calculated for the top solar cell. The remaining part of the spectrum, $E < E_g$ (top), is then used to calculate the performance of the bottom solar cell. In this way, a complete set of isoefficiency curves is generated for various energy bandgap combinations [5,6]. Assuming unity quantum efficiency and no losses, the model predicts a maximum solar cell efficiency of 38.4 percent at AM0 and one sun insolation. This performance is based upon a four-terminal configuration for the tandem stack. Figures 3 and 4 show the predicted theoretical efficiencies for two- and four-terminal tandem solar cells as a function of top₂ and bottom solar cell bandgap for the AMO spectrum (135.3 mw/cm^2). This model predicts the ideal top solar cell in combination with a silicon bottom solar cell. For the two terminal case, the optimum top solar cell bandgap is 1.78eV, and for the four-terminal case, the optimum is 1.97eV.

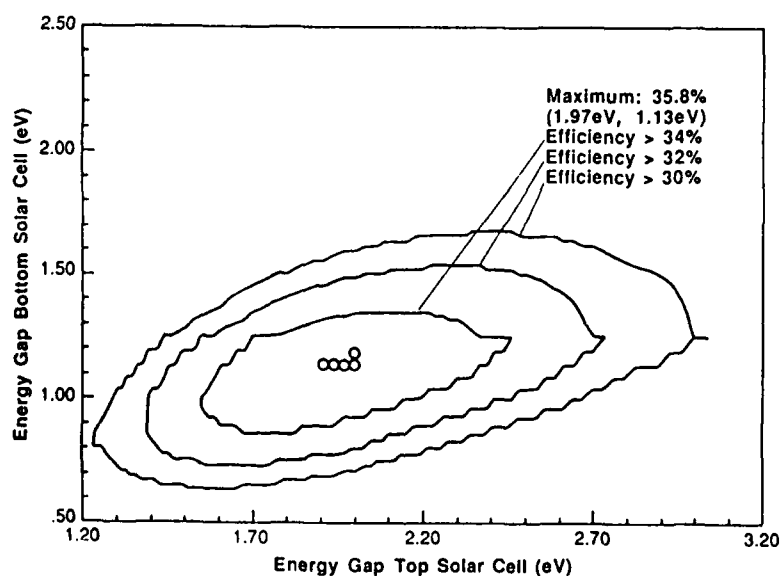


Figure 3. Theoretical Isoefficiency Graph: Top and Bottom Solar Cell Bandgaps for AMO Four-Terminal Configuration, from Nell and Barnett [5].

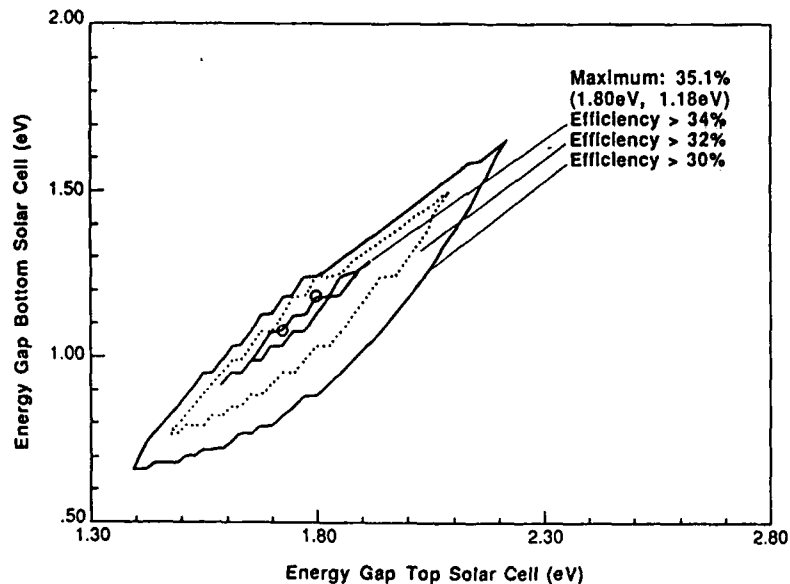


Figure 4. Theoretical Isoefficiency Graph: Top and Bottom Solar Cell Bandgaps for AMO Two-Terminal Configuration, from Nell and Barnett [5].

1.2 Project objectives

The overall technical objectives for the Phase II program have been to design, fabricate and optimize the two-junction tandem structure consisting of GaAsP top solar cells mechanically-stacked on silicon bottom cells in both two- and four-terminal configuration. Improved performance, scale and survivability of space photovoltaic arrays are the expected tangible results of these objectives.

In this report, the tandem solar cell design, the GaAsP top solar cell fabrication, and experimental results are described. Individual solar cell results in terms of open-circuit voltage, top solar cell transparency, short-circuit current, and fill-factor are given. Projection of the combined efficiency of these GaAsP on GaP top solar cells with state-of-the-art Swanson [7] and Green [8] silicon solar cells are given. AMO spectra and device characteristics are cited throughout. This work can be extended to terrestrial concentrator applications.

2. MAIN TEXT

2.1 Description and Discussion of Research Work

The tasks to be performed on this program were divided into the following activities: tandem solar cell design (Section 2.1.1), top solar cell growth techniques (Section 2.1.2), top solar cell design issues (Section 2.1.3), and solar cell testing and characterization (Section 2.1.4). These activities include liquid phase epitaxial crystal growth, junction-formation, metallization and contact formation, tandem cell assembly and measurements and qualification testing of the top cell and the assembled two-junction device. The results achieved are detailed in Section 2.2.

The methodology used for the GaAsP top solar cell development is based on systematic individual, sequential improvement of the tandem solar cell parameters: open-circuit voltage, short-circuit current, fill factor, and transparency below the top solar cell bandgap. The most difficult parameter to achieve for any new solar cell material is the open-circuit voltage [9]. The next most difficult parameter is subbandgap transparency. Short-circuit current and fill factor are individually optimized. When optimum performance is demonstrated for the individual parameters, then the development effort is directed to incorporating these parameters into a single device design and fabrication process.

2.1.1 Tandem solar cell design

In this section, considerations for the design of the tandem GaAsP-Silicon solar cell are divided into the following:

- o Ideal silicon bottom cell expectation.
- o Real bottom solar cell expectation.
- o Predicted top solar cell performance.
- o Expected tandem solar cell performance.

For maximum practical tandem solar cell conversion efficiency, both the top and bottom solar cells must be approaching their theoretical limit. In the case of the bottom solar cell, the maximum efficiency predicted by the refined model for a silicon space solar cell is 26.2 percent at AM0 and one sun [5,6]. Swanson's [7] record efficiency concentrator solar cell is equivalent to 19.9 percent efficient for an AM0 spectrum at one sun, while Green's [8] best result corresponds to an efficiency of 19.7 percent (AM0, 1 sun). These results are 30 percent better than the average commercial silicon space solar cells. Table 1 shows a comparison of these results.

Table 1

Modelled Theoretical Maximum
for Silicon Space Solar Cells
Compared to Actual Silicon Results

	$\frac{V_{oc}}{(\text{volts})}$	$\frac{J_{sc}}{(\text{mA/cm}^2)}$	$\frac{FF}{}$	$\frac{Eff.}{(\%)}$
Model	0.791	53.43	0.840	26.2
Swanson	0.681	50.30*	0.784	19.9
Green	0.653	49.30*	0.829	19.7
Commercial	0.595	46.00	0.750	15.2

*Corrected from AM1.5 global to AM0

For the mechanically-stacked, four-terminal tandem solar cell, the calculated theoretical efficiency of the optimum GaAsP top solar cell is 22.6 percent, as shown in Table 2. (This optimum corresponds to a bandgap of 1.97 eV, and a composition of GaAs_{0.54}P_{0.46}.) Losses may be predicted to obtain the best "real" case. Based on a performance comparison of well-developed solar cells with their expected theoretical limit, one may predict the expected performance of the 1.97 eV GaAsP top cell [9]. Mid-range achievements of open-circuit voltage, short-circuit currents and fill factors are 96 percent, 91 percent, and 96 percent respectively, of the expected limits from the model. This approach of scaling theoretical limits to predict the "real" or "best case" performance has been demonstrated to be valid for all well-behaved solar cells. This is particularly true of the III-V compounds. Using these assumptions, the best case 1.97 eV GaAsP top solar cell should peak at 18.8 percent efficiency, as shown in Table 2.

Table 2
Expectation of Best
Case GaAsP at 1.97 eV

	$\frac{V_{oc}}{(\text{volts})}$	$\frac{J_{sc}}{(\text{mA/cm}^2)}$	$\frac{FF}{}$	$\frac{Eff.}{(\%)}$
Theoretical	1.62	20.75	0.91	22.6
Best Case	1.55	18.90	0.87	18.8
% Theoretical	96%	91%	96%	--

With these expectations of the top and bottom solar cells, one can view the performance of the GaAsP-Si tandem stack. The best case tandem structure with various bottom solar cells is shown in Table 3.

Table 3

Best Case Tandem Solar Cell with
Various Silicon Bottom Solar Cells
(AM0)

	<u>Swanson</u>	<u>Green</u>	<u>Commercial</u>
GaAsP Top Cell	18.8	18.8	18.8
<u>Si Bottom Cell</u>	<u>11.5*</u>	<u>11.4*</u>	<u>8.8*</u>
Stack Eff. (%)	30.3	30.2	27.6

*Includes an extra 5 percent reduction in Jsc due to optical transmission losses.

The performance requirements necessary for achievement of a 25 percent tandem device can be described in terms of transparency, voltage, fill factor and current.

The transparency of the top solar cell determines the overall reduction in performance of the bottom solar cell. This reduction is in the short-circuit current. Allowing for an additional 5 percent reduction due to optical losses, the best state-of-the-art silicon solar cell should be 11.5 percent efficient when placed under a GaAs_{0.54}P_{0.46} top solar cell. Hence, a 13.5 percent efficient top solar cell is needed to achieve the goal of a 25 percent efficient tandem stack.

A comparison of the best case GaAsP solar cell parameters to those required for the achievement of a 25 percent efficient tandem solar cell is shown in Table 4.

Table 4

Comparison of Best Case
GaAsP to Requirements for a 25 Percent
Efficient 4-Terminal Tandem Solar Cell

	<u>Voc</u> (volts)	<u>Jsc</u> (mA/cm ²)	<u>FF</u>	<u>Eff.</u> (%)
Best Case	1.55	18.9	0.87	18.8
Required	1.46	14.9*	0.84	13.5

*Requires total quantum efficiency of 71.8 percent.

2.1.2 Top Solar Cell Growth Technique

In this work, liquid-phase epitaxy was used to grow the basic GaAsP top solar cell structure. Liquid-phase epitaxy has continued to be the process by which the highest quality semiconductor

devices are produced. For example, recent improvements in light-emitting diodes by heterostructure LPE growth methods have resulted in an order of magnitude improvement in brightness. These LED's are now being considered for very high performance applications, such as brake lights in automobiles. The highest efficiency commercial GaAs solar cells are grown by liquid-phase epitaxy [10].

Liquid-phase epitaxial growth of multi-layer structures of GaAs-GaP was performed using the slider method [11]. The slider apparatus serves as a substrate holder and melt container for the metallic growth solutions. Advantages of the slider apparatus over other techniques, such as dipping, are 1) the substrate wafer can be brought in and out of contact with the melts, 2) several melts can be used in sequence, 3) growth is restricted to a single side of the wafer, 4) substrate-solution contact is from the bottom of the melt where there are no floating oxides or other contaminants, 5) excess solution can be wiped off the wafer by the slider action of the boat, and 6) thermal equilibrating and temperature profiling are greatly facilitated. The graphite slider apparatus fits into a cooling or temperature gradient furnace, as appropriate. The furnace zones can be controlled to better than 1°C . We use a furnace atmosphere of palladium-diffused hydrogen, which is continuously sweeping the furnace and slider apparatus during the furnace operation.

A feature of the slider boat apparatus particular to this program is the grading of the width of the growth wells shown in Figure 5. This graded well width design permits individual access to each of the grown layers after the substrate is removed from the boat.

Growth is accomplished by placing the GaP substrates under the first melt to grow a transition layer of $\text{GaAs}_x\text{P}_{1-x}$ by controlling the temperature level, cooling rate, and time of exposure, and continuing, in turn, to each melt shown in the growth apparatus in Figure 5 until all requisite layers are grown.

Material evaluation in terms of layer thickness and composition growth morphology is accomplished by optical microscopy and/or scanning electron microscopy.

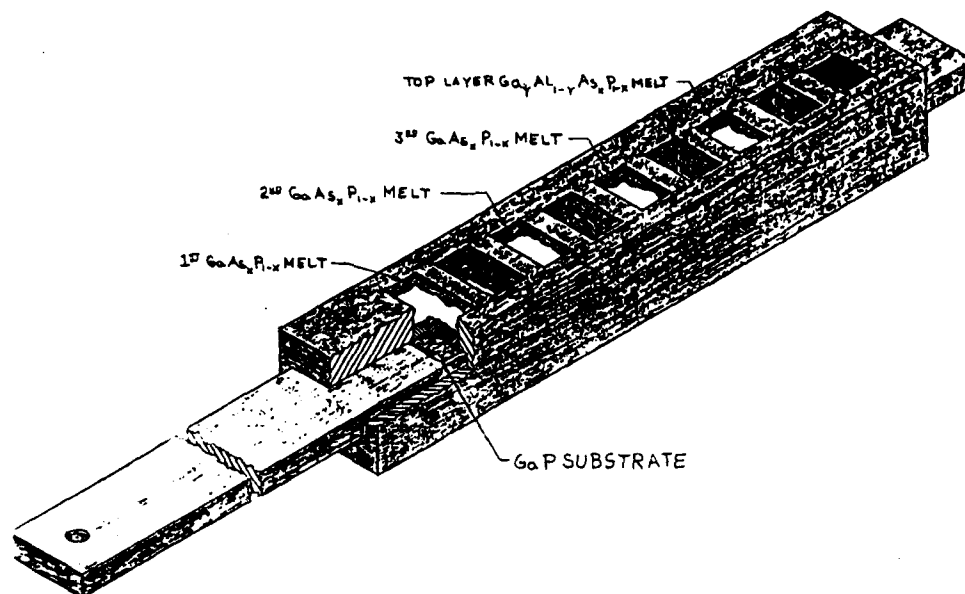


Figure 5. Slider boat growth apparatus showing the graded well width.

Figure 6 shows a typical GaAsP top solar cell structure.

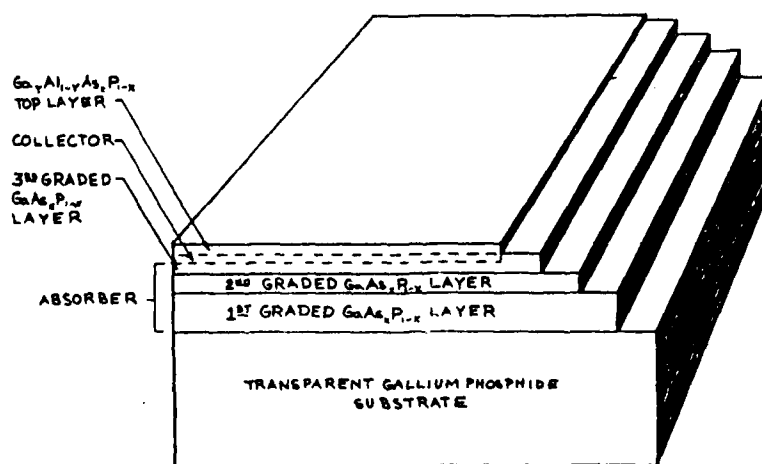


Figure 6. GaAsP on GaP solar cell structure (not to scale).

The main growth variables -- growth time, temperature level, growth rate and melt size -- can be varied based on detailed comparison of the experimental results of the model. Initial and final temperature and melt compositions establish the grown layer composition. Melt size and wafer area determine layer thickness. Cooling rate and growth time are dependent on each other since

initial and final temperatures are fixed for a given growth situation. For example, slowing the actual growth rate may be used to improve crystal morphology, leading to increased growth time. Improved surface morphology was accomplished by careful substrate cleaning, the use of supersaturated melts, zirconium melt additions, growth interrupt techniques, and by bismuth-graded interlayers. (See extended discussion at the end of this section.)

The cap layer, in some cases, was also a thin grown layer. The cap serves to reduce surface recombination, and it can also serve as a source of dopant for a diffused junction [12]. This layer was either GaP or $\text{Ga}_y\text{Al}_{1-y}\text{As}_x\text{P}_{1-x}$ material with initial experiments using gallium phosphide. In later experiments $\text{Ga}_y\text{Al}_{1-y}\text{As}_x\text{P}_{1-x}$ cap layers were investigated to reduce interface dislocations due to the GaP lattice mismatch. Cap layers were also prepared by techniques other than liquid-phase epitaxy. (See Section 3.1.3.3)

Devices were fabricated from an AlGaAs/GaAs structure grown on a GaP substrate by LPE. This structure incorporated the largest lattice mismatch possible in the GaAs-GaP system. A series of growth stops were used to minimize the propagation of dislocations. A smooth, mirror-like surface resulted from this growth process, and open-circuit voltages up to 0.909 volts were observed. Clearly, if compositional grading is done properly and the propagation of dislocations minimized, J_0 can be minimized, and therefore voltage maximized, in lattice mismatched systems. The effect of grading procedure on dislocation density and electrical performance in GaAsP (1.75 eV) has been studied by Wanlass [13]. Extrapolating Wanlass's results to the case of GaAs on GaP is accomplished in the Table 5, as follows.

Table 5

Predicted Open-Circuit Voltage for GaAs on GaP
with Variable Gradings and Defect Structure

Grading Process, Thick. -----	Dislocation Density [13]		Open-Circuit Voltage (volts)		
	Threading	Misfit	GaAsP [13] (1.75ev) -----	GaAs/GaP Theory -----	Best Case -----
Contin., 8 microns	8×10^5	0	1.244	0.976	0.937
10 layers, 9 microns	6×10^5	0	1.230	0.965	0.926
5 layers, 8 microns	7×10^5	0	1.241	0.972	0.933
5 layers, 4 microns	2×10^6	0	1.230	0.964	0.925
3 layers, 8 microns	2×10^6	2×10^2	0.666	0.523	0.502
2 layers, 8 microns	2×10^6	4×10^2	0.332	0.261	0.250
1 layer, no grade	2×10^7	1×10^3	0.331	0.260	0.249

Therefore, the measurement of $V_{oc}=0.909$ volts is entirely consistent with a graded structure containing $2 \times 10^6/\text{cm}^2$ threading dislocations and the termination of misfit dislocations.

Featureless layers of high GaAs content on GaP substrates may be prepared by the use of growth-interrupts and bismuth melts. The growth interrupt procedure was found to be useful in terminating dislocation loops in the lower layers of a multilayer structure. Bismuth melts have a particularly useful GaAs-GaP solubility relationship that lead to very effective compositional-grading layers. A typical bismuth-grading layer profile determined by SEM-EDS is shown in Figure 7.

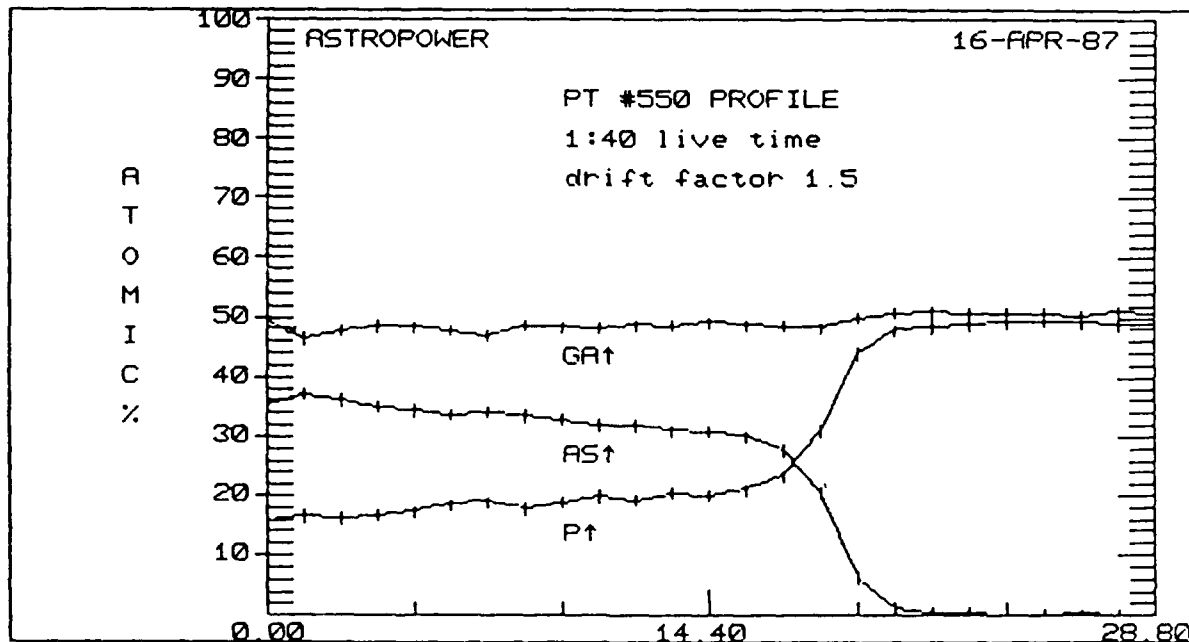


Figure 7. Compositional profile of an edge cleave of a bismuth-graded GaP-to-GaAs LPE layer growth. Micrograph is by SEM-EDS technique.

Improvements in growth morphology and device quality have also resulted from deliberate metallic zirconium additions to the LPE growth melts. This technique was suggested in the work of Chang, Meng, and Stevenson [14]. The specific results which indicate improvements for the zirconium additions are, as follows:

- o Reduced LPE system oxygen level resulted in improved growth morphology, more-planar layers, and fewer stacking faults.
- o Undoped GaP LPE runs are low carrier-concentration p-type, similar to GaAs LPE work reported in the literature where deep oxygen donor levels are removed.
- o Photoluminescence of GaP LPE runs with metallic Zr additions is peaked in the green, whereas undoped GaP without Zr peaks in the red. This indicates that the Zr is preventing oxygen contamination of the GaP layer during growth.
- o MIS device results for 2.15 eV GaAsP layers indicate a short-circuit current density that is better than previous-high values for 2.07 eV GaAsP. On an equivalent bandgap and composition basis, this is projected to be at least a 20 percent improvement.

Zirconium gettering during LPE growth is important for reducing system oxygen levels and improved solar cell performance. This technique was used in all LPE runs in the last three months of this program.

2.1.3 Solar Cell Device Issues

The experimental fabrication methodology for this program has been to sequentially demonstrate each top solar cell performance factor:

- o Subbandgap Transparency, including substrate
- o Voltage, operating and open-circuit
- o Current
- o Fill-Factor and Power Efficiency

The individual refinements would, then, be combined into a single optimized GaAsP top solar cell.

Summary -- Top Solar Cell Device Issues

The original focus was on transparency and open-circuit voltage because these parameters are the most difficult to maximize with a new solar cell design [9]. Optimization of the p/n junction formation technology described below led to the demonstration of a top solar cell with the values for those parameters as follows: Transparency = 95 percent; Voc = 1.397 volts; FF = 0.81. Short-circuit currents were low on junction solar cells made during this phase of the program. The maximum current density was 6.02 mA/cm², which led to an overall efficiency of 5.1 percent.

To increase Jsc, the focus shifted from junction devices to MIS structures. This approach led to an improvement in energy conversion efficiency from the 5.1 percent reported in mid-1986 for a p-n junction solar cell to the 10.6 percent reported in early 1987 for an MIS solar cell. The highest efficiency MIS device had a Voc of 0.901 volts and a Jsc of 19.8 mA/cm².

At this stage MIS and ITO device structures were used as test vehicles since they eliminate or minimize the effects of surface recombination and the junction formation process on the current. We are able to fabricate and test these device structures with rapid turnaround, leading to efficient feedback of device results into the materials growth program.

The MIS and ITO devices exhibit lower voltages than the p/n junction. Early MIS open-circuit voltages were observed from 0.23 volts to 0.86 volts. In spite of these low voltages, we were able to achieve an improvement in overall efficiency with the best devices. The characteristics of the best single device (Area: 0.1 cm²) follow:

Bandgap	1.78 eV
Voc	0.901 volts
Jsc	19.8 mA/cm ²
FF	0.80
Efficiency	10.6%

There were three problems with the MIS solar cell. First, we have been unable to achieve high voltages on this two-terminal device. This problem can probably be solved with the development of a proper insulating layer. The second problem is the scaling to larger areas. Local defects affect device performance greatly with full-coverage contacts in the MIS devices. The third problem is performance degradation upon antireflection coating the MIS solar cell.

During this work, a very high value of Voc of 1.318 volts was achieved for a wide bandgap GaAsP solar cell using antimony trioxide. A Sb₂O₃ sputtering target for the I-layer was specified and ordered to solve the problems with the MIS device. The target was not thermally or mechanically stable, and "fell apart" under moderate sputtering conditions. The vendor, Cerac, agreed to replace it, but was unable to develop a process that will give us a durable target during the program.

At this stage the basic question is whether the high currents can be retained when returning to junction devices. Our results with GaAs indicate that this should be possible. We have measured a current density of 28.6 mA/cm² on a ITO GaAs structure. A GaAs p/n junction device using material from the same growth gave a current density of 27.3 mA/cm². This apparent reduction in current of 4.5 percent is well within acceptable limits.

Accordingly, the fabrication program focus was switched back to the p-n junction. A new p-n junction solar cell design was developed. The essence of the new design is in the thin emitter and the elimination of punch-through from the top contact to the device junction. The GaAsP top solar cell technology has been limited, in the past, by these two factors. AstroPower has demonstrated the fabrication processes needed for achieving individual parameters in the new top solar cell design under this contract. The design is based on a set of simple, reliable process steps. Close tolerance steps have been eliminated. This design solves many of the problems of obtaining the high MIS device currents while also achieving the higher voltages and uniformity of p-n junctions. This new design of the GaAsP top solar cell with thin emitter/top contact is clearly superior to previous GaAsP top solar cell designs. This new design is applicable to a number of high performance space solar cells and is described in Section 2.1.3.4.

2.1.3.1 Subbandgap Transparency

The transparency of GaAsP/GaP samples were measured with and without antireflection coatings during this contract. With uniform growth morphology and planar structure, it was possible to achieve over 95 percent subbandgap transparency in most samples tested. This corresponds to approximately 60 percent overall transmission, depending on the top solar cell bandgap.

In the optical measurements, transmission is defined as the percentage of Jsc measured from a Si "space" cell when illuminated through the test sample as a filter element. GaAsP transmission as high as 59.8 percent was measured even with a non-optimized SiO_x antireflection coating.

As an example of this work, three GaAsP/GaP samples (PT#80S, PT#80D, and HO#110) were tested. The transmission data are, as follows:

Sample	No AR	Methanol Between	Methanol Between & Top SiO _x AR
PT#80D	27.5%		
PT#80S	31.7%	37.4%	40.6%
HO#110	35.4%	41.2%	43.9%
			59.8%

The light used for these measurements was a General Electric ELH bulb, operated at 100 VDC and filtered through a Schott KG2 filter. The samples were prepared by an aqua regia etch of both faces: some texturing of the Ga <111> face was observed in all samples. Reflection and transmission spectra were collected for samples PT#80D (LPE film grown on the P <111> face), and PT#80S (LPE film grown on the Ga <111> face). These data indicate that the bandgap of both samples was 2.12 eV. The bandgap of the HO#110 filter was estimated to be 2.09 eV based on composition. This sample was antireflection coated with 700-800 Angstroms of thermally evaporated SiO_x on both faces.

The 59.8 percent transmission that was observed in HO#110 is equivalent to 95 percent transparency to photons less energetic than the GaAsP bandgap.

In summary, high subbandgap transparency of the GaAsP/GaP material was demonstrated early in this contract.

2.1.3.2 Voltage, Operating and Open-Circuit

The following section describes the experimental work to enhance solar cell voltages in p-n junction solar cells during the first year of the contract and after the major MIS device work was completed in July 1987:

- o Solid-state diffusions with silica-solid dopant thin film layers.
- o Grown junction by incorporation of appropriate dopants in the LPE melt.
- o Vapor diffusion doping with control of active-layer surface decomposition.

Solid-State Diffusions -- Reproducibility of solid-state diffusions of zinc to form the emitter layer depends on the exact nature of the base SiO_x layer. The process entails a "zinc source" sandwich between two other layers. The layer between the "zinc source" and the substrate is the buffer layer and the top layer serves as a cap layer. It has been determined that an E-beam evaporated SiO_2 buffer layer leads to fewer defects than a thermally evaporated SiO_x layer. The base SiO_x layer is required to get planar Zn_3P_2 layers; Zn_3P_2 will not deposit uniformly on the GaAsP surface.

The diffusions using silica- Zn_3P_2 produced open-circuit voltages of 1.37 to 1.39 volts for areas less than 0.1 cm^2 . E-beam evaporated SiO_2 is stoichiometric (SiO_2 instead of SiO_x) and appears to be more of a diffusion barrier than the thermally-evaporated SiO_x layer. We have concluded that uniform, consistent Zn_3P_2 layers are possible when the base SiO_x layer is controlled and that the solid-state diffusion can be reproduced with appropriate control of the respective layers.

Solid-state diffusions were also attempted with other dopants, Cd_3P_2 and Mg_3As_2 . Two Cd_3P_2 experiments resulted in no net penetration of the GaAsP at temperatures up to 850°C for 30 minutes. The Mg_3As_2 exhibited a very low degree of wetting on the silica base, even with a cap layer, and it was not possible to construct a planar, continuous film of Mg_3As_2 to effect a controlled solid-state diffusion.

The Zn_3P_2 solid state diffusions give high values for open circuit voltage. There are indications that solid state Zn_3P_2 diffusion to form the shallow emitter junction has been leading to "dead" layers. This is consistent with observations made by others in GaAs [15]. Attempts to remove these "dead" layers by thinning with successive anodic dissolutions or by annealing (to drive the zinc from interstitial sites into substitutional sites) did not result in short-circuit current improvements.

Grown Junctions -- Voltages as high as 1.51 volts (PT #214) (GaP p/n) have been obtained with grown junctions by preparing the n-type and p-type layers in separate runs. In the case of grown emitters (GaP p/n devices), the problem of controlling zinc doping is limited by the vapor pressure of zinc itself. With the p-on-n devices, three different p-type dopants were investigated: Zn,

Mg_3N_2 , and Mg_3As_2 . Of these, Mg_3As_2 appear to give the best results. Best Voc's were 1.42 volts for Mg_3As_2 doping compared to 1.37 volts for Mg_3N_2 doping. We obtained 1.51 volts with Zn doping on #214, but Mg_3As_2 appears to be more consistent.

For n-on-p devices, the p-layer was Zn doped and the n-layer was Sn or Te doped. That is, the n-layer was grown from a tin melt ($5 \times 10^{18}/\text{cc}$) and Te was used as an additional dopant. The best Voc for n-on-p devices was 1.379 volts. These samples showed a reverse bias breakdown greater than 10 volts which indicates good material quality.

Both the n-on-p and p-on-n GaP devices showed low current. Spectral response was determined on #214 (Zn doped p-on-n), #267 (Mg_3N_2 doped p-on-n), #268 (Mg_3As_2 doped p-on-n), and commercial Sumitomo LED material. Of these, the only sample to show the indirect bandgap response was the Sumitomo sample. The other grown devices showed spectral responses in the region corresponding to the direct bandgap (2.78 eV). The basic difference between these samples is the fact that the Sumitomo samples had a 20-micron emitter and was nitrogen doped, while the other samples had 1-micron emitter and no nitrogen doping.

Grown junctions were prepared with beryllium, magnesium, and zinc doping. Minimum layer thicknesses were approximately 1.5 microns, so low currents were to be expected. Of these three dopants, zinc gave the highest value for open-circuit voltage (1.51 volts for #214). Grown emitters doped with Mg and Be were substantially lower in open-circuit voltages, but it is difficult to know the p-layer doping concentration of the thin layers and the Be or Mg emitter doping levels were not optimized. Attempts to solid-state diffuse magnesium are suggested for future work, because magnesium will diffuse slower than zinc, and magnesium diffusions are not site, stoichiometry, or concentration dependent. This means that magnesium should be less prone to form "dead" layers and lends itself to controlled shallow diffusions that are not stoichiometry or concentration dependent.

Vapor Diffusion -- Other possible techniques for forming the p-type emitter layer were considered. Ampoule diffusion from zinc vapor from the sublimation of either pure zinc or zinc compounds with arsenic or phosphorus has been used for commercial light-emitting diodes. The problem with this process is the high level of surface damage ("white plague" in the LED industry) induced by the zinc surface concentration. LED's have been tolerant of this process because the optimized LED junction depth is 1.8 - 2.3 microns, and the surface damage can be removed by light etching after the diffusion step.

A direct zinc vapor-diffusion technique into the GaAsP has been worked out during this program. Diffusion apparatus modifications have resulted in no surface decomposition and controlled

zinc surface concentrations during diffusion. Devices having 2 cm. x 2 cm. geometries were diffused late in the contract. Open-circuit voltages up to 1.43 volts were measured on solar cells fabricated by this technique. Short-circuit currents vary with the diffusion condition and ultimately the junction depth. The best devices were diffused at 650°C for five minutes and resulted in $V_{oc}=1.409$ v, $J_{sc}=7.7$ mA/cm².

The improvements in voltage during this contract are shown in Figure 8.

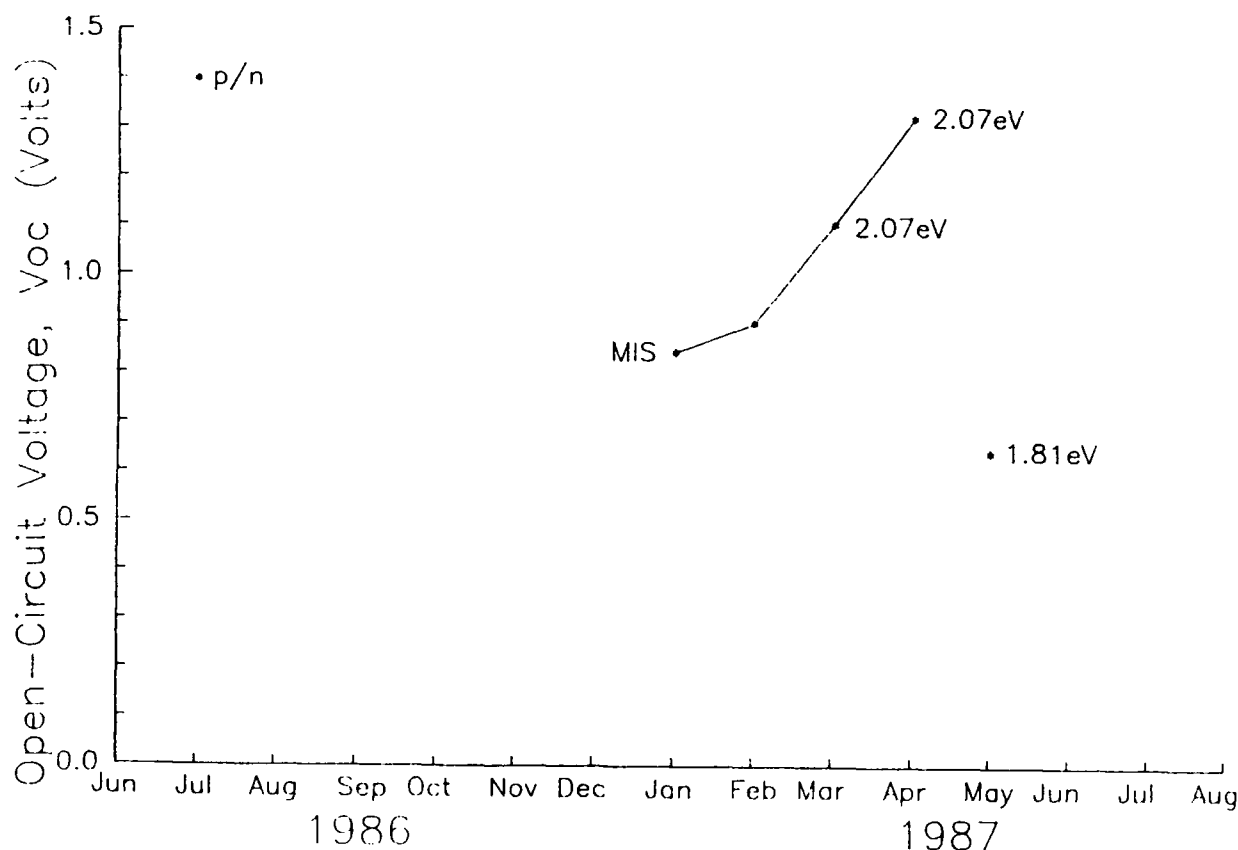


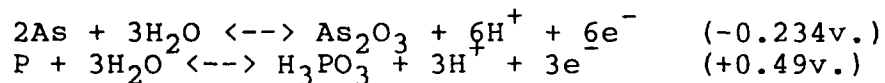
Figure 8. Improvements in Voltage during this Contract.

2.1.3.3 Current

The experimental part of the research to improve top solar cell currents, both operating and short circuit (J_{sc}), are described in this section. Emitter thinning, isoelectronic doping, MIS device preparation, and heterostructure cap layer confinement were the approaches used to achieve current levels in the top solar cells which were as high as 80 percent quantum efficiency.

Emitter thinning -- During this program the diffused emitter layers were thinned by anodic dissolution techniques. Anodic oxides can be grown on GaAs, GaP, and all GaAsP active layers without difficulty. The process is very controllable and can remove quite precise thicknesses of material. The anodic oxide growth appears to passivate the surfaces of some samples resulting in significant increases of Voc. The oxide grown is transparent and could serve as part of a multilayer AR coating or cap layer.

It is evident, at this time, that the anodic dissolution of the GaAsP layer is slower than GaAs or GaP by themselves. The GaAsP dissolution process is sensitive to local surface damage near the contacts. This is probably due to the gold-based contact metallization. B. Schwartz [16] describes the oxidation of arsenic and the oxidation of phosphorus to be quite different:



Some typical results are shown in Table 6. It appears that the most desirable technique would be to anodize completed cells in a test, anodize, test iteration to maximize Isc; however, the gold-Zn contact will not survive the process. One of two effects are observed on every sample with exposed metal contacts: 1) the contacts are removed or 2) anodic etching rather than oxide growth takes place. The anodic etching causes severe surface damage.

Table 6

Anodic Thinning of GaAsP Samples

Sample H050786B was thinned prior to contacting by three 140 V anodization steps (All cells 0.109 cm²)

<u>Cell #</u>	<u>Voc (v)</u>	<u>Isc (mA)</u>	
1	1.330	0.38 mA	
2	1.385	0.38	
3	1.319	0.38	tested before alloy step
4	1.404	0.38	
5	1.405	0.35	
6	1.405	0.35	

Sample H050786A thinned prior to contacting by two 140 V anodizations and five 120 V anodizations

<u>Cell #</u>	<u>Before Alloy</u>		<u>After Alloy</u>	
	<u>Voc (v)</u>	<u>Isc (mA)</u>	<u>Voc (v)</u>	<u>Isc (mA)</u>
1	1.335	0.32	1.382	0.34
2	1.319	0.20	1.369	0.20
3	1.295	0.30	1.347	0.32
4	1.320	0.20	1.376	0.30
5	1.136	0.30	1.216	0.28
6	1.153	0.28	1.227	0.25

Sample H041886 IIA was finished then anodized by careful masking of grid with black wax.

	<u>Cell</u>	<u>Voc</u>	<u>Isc</u>
Initial	1	1.172	0.30
	2	1.383	0.30
2 120 V anodizations	1	0.162	0.34
	2	1.400	0.34
3 120 V anodizations	1	1.161	0.37
	2	1.412	0.46
3 120 V anodizations	1	1.134	0.38
	2	1.364	0.18

Nitrogen Isoelectronic Doping Effects -- Nitrogen doping is a possible method for increasing photon absorption and short-circuit current at the high bandgap (or high percent GaP) end of the GaAsP composition range. From Bachrach [17], Figure 9 shows the difference in optical absorption for GaP with and without deliberate nitrogen doping. This implies that GaP can be made "quasi-direct" by isoelectronic doping.

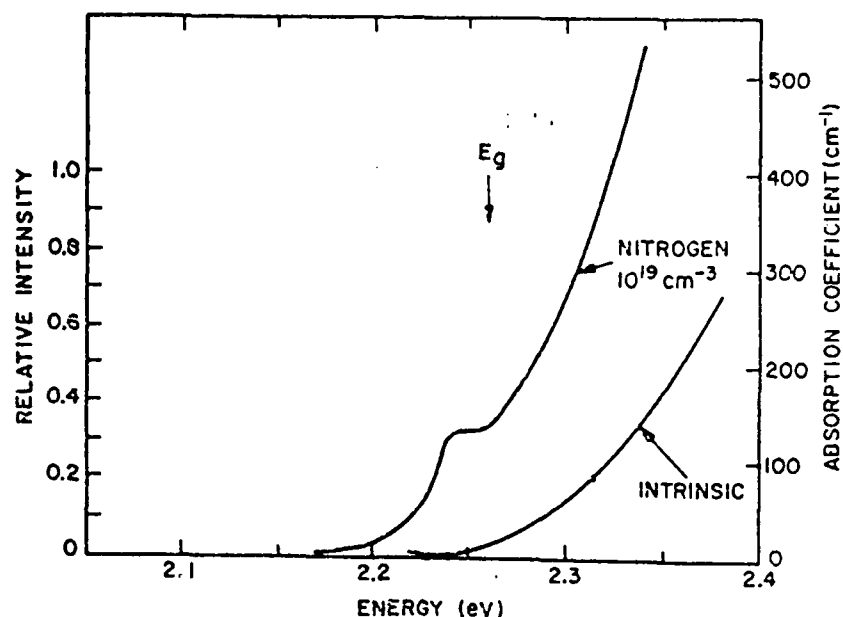


Figure 9. Optical Absorption Spectra of GaP with and without deliberate Nitrogen Doping.

Nitrogen doping by addition of gallium nitride to the LPE melt was attempted, but nitrogen incorporation was minimal and the surface morphology was noticeably poorer in the presence of the gallium nitride. We conclude that the solubility of GaN in the metallic solvent was not sufficient at the growth temperature used.

Nitrogen-doped GaP structures, using gas-phase ammonia additions, have exhibited high quality, planar morphologies. However, initial runs with NH_3 had no or, at most, dim red photoluminescence response. Addition of zirconium to getter oxygen resulted in a coating on the melt which blocked the incorporation of the nitrogen. We eliminated this problem by pre-charging the melt with nitrogen and then adding zirconium as a second step. Photoluminescence of this material shows a strong green peak indicating that the oxygen is being removed and that the nitrogen is being incorporated in the semiconductor lattice.

Nitrogen doping must be carried out with low oxygen levels to be effective. A strong green photoluminescent response results when the LPE growth is oxygen-gettered by Zr addition. The sequence of N and Zr additions is very important. In this work the desired shift in bandedge, and increase in photon absorption, was observed with nitrogen-doped gallium phosphide. However, the minority carrier diffusion length appeared to be reduced with added isoelectronic dopant.

In experimental work with another potential isoelectronic dopant, bismuth, surface morphology and open-circuit voltages were clearly reduced by the addition of bismuth to the LPE-grown solar cell structure.

Heterostructure Cap Layers --Cap (or "window") layers have been prepared by two possible processes: LPE grown layers or flash-evaporated layers.

Grown cap layers were briefly discussed in the LPE section above. Lattice-mismatched cap layers (e.g., GaP on the top active GaAsP layer) were explored during this contract. Cap layers must be close to lattice-matched so that nucleation of the grown layer is not inhibited locally, leading to differences in junction depth in the subsequent diffusion depending on whether the dopant source is solid-phase (grown-layer) or liquid-phase (melt). Stress/strain from cap layer lattice mismatch must be isolated from the thin emitter layer and junction. These two basic problems have led to the recommendation that future work should be done on lattice-matched cap layers. A further constraint is that, if the composition of the cap layer is considerably different from the adjacent material, e.g., the emitter layer, the melt chemistry may cause some meltback of this layer.

Passivation of GaAs surfaces by amorphous phosphorus overlayers have been described by Olego, Schachter, and Bauman [18]. The technique for flash-evaporated gallium phosphide, as a cap layer, was investigated late in the contract. Conditions were investigated for improved coating adhesion, reduced surface decomposition, the proper level of substrate heating during flash evaporation, and control of the gallium phosphide stoichiometry during evaporation. This work should continue as part of a future program to reduce surface recombination in this material system.

The improvements in current collection during this contract are shown in Figure 10.

The experimental strategy for this program has been to maximize short-circuit current by fabrication of LPE-grown layers of candidate materials into MIS solar cells for quick evaluation of the grown layer quality. In addition, devices were made with conducting indium-tin-oxide (ITO) top contacts to achieve quicker Jsc evaluation than is possible with the MIS test devices. A added advantage is that the ITO coating can be removed making it possible to form p/n devices after Jsc qualification.

These MIS Jsc results as a function of active region bandgap (or composition) are summarized in Figure 10. The GaAsP layers in Runs #368 and #369 were doped with Mg_3N_2 and have given the best 1.97 eV results to date.

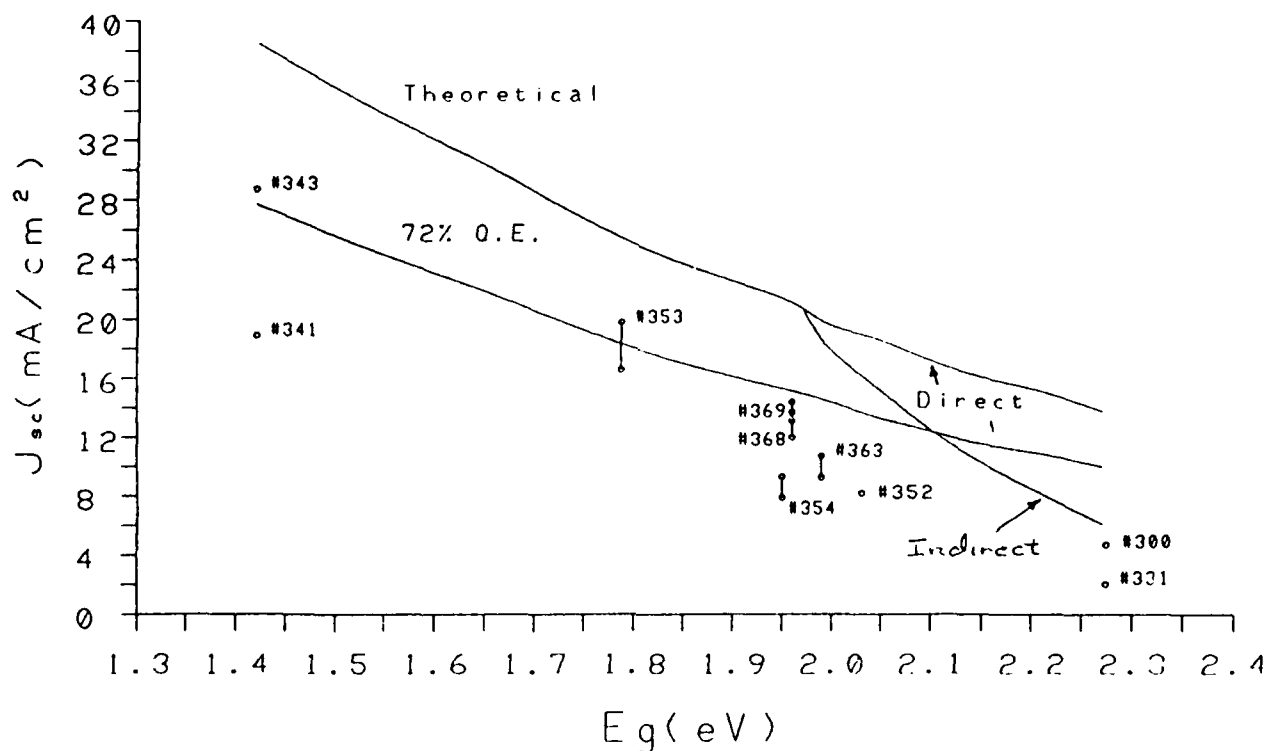


Figure 10. Short-circuit current for MIS devices as a function of GaAsP bandgap. Theoretical line corresponds to unity quantum efficiency. 72 percent Q.E. line is the target J_{sc} for 25 percent tandem cell efficiency.

2.1.3.4 High Performance Design

The high performance GaAsP top solar cell design has been specified and is described in detail in this section.

The features of this design include:

1. GaP substrate that is transparent to photons below the GaAsP bandgap.
2. High current generating GaAsP layer grown on the GaP.
3. Thin (500 Å) GaP heteroface cap layer grown on the GaAsP with a simultaneous shallow (100 Å) junction diffusion into the GaAsP.
4. Thin selective metallization (60 Å, 2 percent of the area) over the thin GaP to form a shorting path to a transparent conductor.

5. Transparent conductor such as antimony-doped tin oxide or boron-doped SiC deposited over the selective metallization.
6. Coarse grid metallization (top and bottom) to match the shading pattern of the Si solar cell metallization.

The high performance GaAsP top solar cell design is shown in Figure 11.

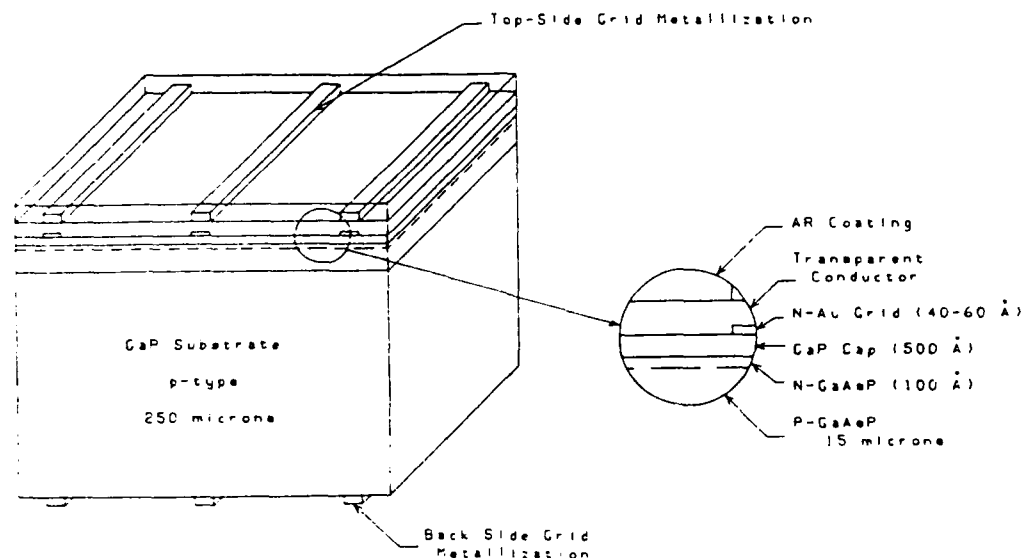


Figure 11. High Performance GaAsP Top Solar Cell.

The design is based on a set of simple, reliable process steps. Close tolerance steps (such as critical metallization times to prevent contact punch-through) have been eliminated. Process Steps 1,2,3,5, and 6 have been completed under this Air Force contract. Process Step 4 has been demonstrated and will be integrated with the other steps.

Following is a brief description of the features of each of these process steps:

1. Gallium Phosphide Substrate -- Transparency of the GaP substrate must be close to 100 percent for photons less energetic than the top solar cell bandgap. We have demonstrated over 95 percent transparency at photon energies less than 1.75 eV for the overall structure.
2. GaAsP Current Generating Layer -- Liquid phase epitaxial techniques have been developed to compositionally-grade from the GaP substrate to the desired bandgap and to provide a constant

composition current-generating layer for the tandem solar cell. We have demonstrated high quality GaAsP layers with short-circuit currents that were up to 80 percent of the theoretical quantum efficiency for a range of bandgaps from 1.78 to 2.15 eV. A quantum efficiency of 72 percent is required for a 25 percent tandem structure. Specific features of this epitaxial growth system that contribute to these results are melt depletion, zirconium gettering, and growth interrupt techniques. Nitrogen doping increases photon absorption of high GaP compositions which would normally act as indirect material. The LPE process is readily scaleable to larger wafer and solar cell sizes. Photoluminescence has been developed as a LPE layer quality assurance technique for this stage of fabrication.

3. Heteroface Cap Layer -- This GaP layer is grown directly on the previous GaAsP layer using close-spaced vapor transport (CSVt). Thin layers, approximately 500 Angstroms thick, have been demonstrated which are less than the coherence thickness for the GaP/GaAsP lattice mismatch. (This means that the layer thickness is less than the critical thickness where the layer will resolve the lattice mismatch stress by spontaneously generating misfit dislocations.) In addition, the cap layer is highly doped with tellurium at 5×10^{18} . This doped layer is the source for a diffused thin emitter layer. The emitter is diffused into the GaAsP during the cap layer growth. The thickness of the n/p emitter is controlled to about 100 Angstroms by the growth temperature, time and doping levels.
4. Cap Metallization Layer -- A thin metal layer is applied to the cap layer to form a shorting contact to the next layer. The metal thickness is 40 to 60 Angstroms and the area coverage is from 2 to 5 percent of the overall device. Punch-through of the exceedingly-thin cap and emitter layers is eliminated by this design. The limited thickness of the metal also leads to less than 1 percent photon loss due to this part of the contact system.
5. Transparent Conductor -- This layer consists of an optically-transparent sheet material over the entire top surface of the cap layer, which transfers current from the thin emitter-cap metallization for eventual collection by the top metal grid. AstroPower has demonstrated tough transparent top-contact materials. Antimony-doped tin oxide and boron-doped SiC are being used since they demonstrate long-term stability and reliability, in contrast to the more traditional indium-tin-oxide transparent conductor material.
6. Top and Bottom Contact Grid Metallization and Antireflection Coatings -- State-of-the-art metal contacts are applied to the top and the bottom of the tandem solar cell in a grid

array that matches the grid on the top of the silicon bottom solar cell. Accordingly the top solar cell does not lead to increased grid shading. Antireflection coatings for both top and bottom of the top solar cell are designed to minimize reflection losses in the tandem solar cell system. We have demonstrated this top and bottom contact and antireflection coating design and application capability under this contract.

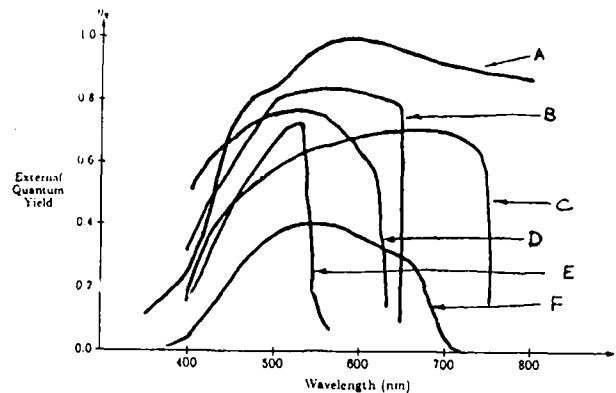
In summary, the parameters, structure, and technology are all in hand for the development of this next-generation space solar cell design. AM0 conversion efficiencies in excess of 25 percent can be achieved. The integration of the technology that has been developed will lead to the demonstration of this new high performance tandem solar cell system.

2.1.4 Solar cell testing and characterization results

The quantum efficiency of the two GaAsP top solar cells (#PT368 and #PT749) has been compared to a gallium arsenide standard, a recent AlGaAs on AlGaAs top solar cell, and two earlier GaAsP structures (#H041886 and #PT184). Figure 12 shows the spectral response of the six samples. Sample #PT184, a p/n cell prepared early in the contract, has a 1.84 eV composition and shows a low quantum yield and a flat response. It is believed that part of this low yield is due to a dead layer resulting from the diffusion process. Another early sample #H041886 has a 2.08 eV composition and peaks in the region corresponding to the direct bandgap. Hence, some efficiency is lost in the indirect composition region.

To achieve the 71.8 percent quantum efficiency needed for the attainment of a 25 percent tandem solar cell, the flat response demonstrated with PT#184 had to be brought up to the level of the H041886 peak. This, indeed, was accomplished with PT#368 and PT#749. Sample PT#368 was an MIS solar cell, grown using step-grading and Mg_3N_2 doping. Sample PT#749 is a p/n device (1.63 eV) grown by the more-recent "quick grade" LPE technology. Both samples show over 70 percent quantum efficiency. A recent AlGaAs on AlGaAs top solar cell result is shown for comparison and achieved over 80 percent quantum efficiency.

Figure 12 demonstrates the improvements during this program in the lattice-mismatched GaAsP on GaP system, and the relative development status of lattice-mismatched (GaAsP on GaP) and lattice-matched (AlGaAs on AlGaAs) technologies.



- A) GaAs p/n homojunction for reference.
- B) AlGaAs on AlGaAs top solar cell.
- C) PT#749 using "quick grade" technology.
- D) PT#368, 1.95 eV GaAsP on GaP solar cell using 4-melt, step-grade and Mg_3N_2 doping.
- E) Sample H041886, 2.08 eV composition.
- F) PT#184

Figure 12. Spectral Response of GaAsP (and AlGaAs) Top Solar Cells, Compared to GaAs Space Solar Cell.

All four solar cell parameter goals (open-circuit voltage, short-circuit current, fill factor, and top solar cell transparency) have been met individually. The following table (Table 7) lists the best individual parameters achieved, and the target for these parameters for GaAsP top solar cells, leading to a 25 percent tandem system.

Table 7

Best GaAsP on GaP Solar
Cell Parameters

	Target	Actual
Transparency, $< E_g$ (%)	95	95
Voc (volts)	1.46	1.43
Jsc (mA/cm^2)	14.9	14.5 (1.95 eV)* 19.8 (1.78 eV)*
FF	0.84	0.84
AMO Efficiency (%)	13.5	10.6

*MIS or ITO Device

The best individual GaAsP top solar cell, combined in a single device, has achieved 10.6 percent. The individual parameters were Voc=.901 volts; Jsc=19.8 mA/cm^2 ; FF=0.8; this device was an MIS device. An increase in voltage of 27 percent to 1.15 volts will lead to an efficiency of 13.5 percent.

Progress in the development of the best top GaAsP solar cell is summarized in the following table:

Table 8

Top GaAsP Solar Cell Progress

		<u>Voc</u> (volts)	<u>Jsc</u> (mA/cm ²)	<u>FF</u>	<u>Eff.</u> (%)
Aug.	86	1.397	6.02	0.81	5.0
Jan.	87	.842	19.8	0.75	9.2
Feb.	87	.901	19.8	0.8	10.6

The first experimental mechanically-stacked two-junction, four-terminal tandem solar cells with a GaAsP top solar cell on a conventional silicon bottom solar cell have been prepared. Figure 13 shows a demonstration mechanically-stacked tandem solar cell. The demonstration cell was 4 cm² in area. The grid patterns are aligned to minimize optical transparency losses to the silicon bottom cell.

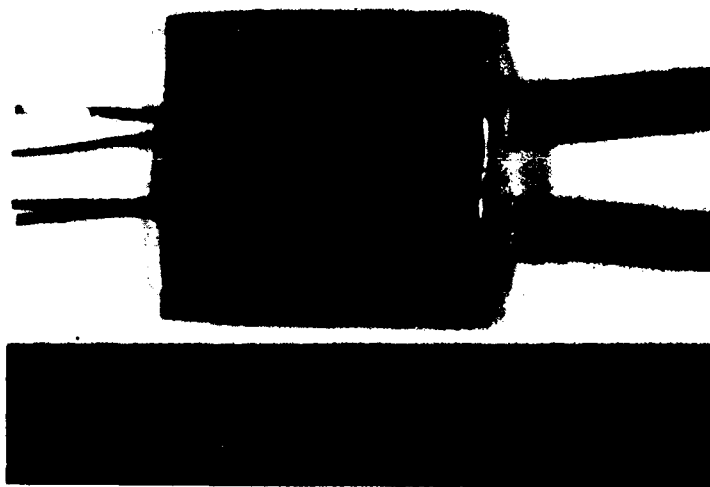


Figure 13. GaAsP/Silicon Mechanically-Stacked, Four-Terminal Tandem Solar Cell, 4.0 cm².

Development of the GaAsP top solar cell has resulted in top solar cells with 10.6 percent energy conversion efficiency. Individual optimization of open-circuit voltage, top solar cell transparency, short-circuit current, and fill factor has led to a top solar cell device which, when combined with state-of-the-art silicon bottom solar cells, will achieve the overall tandem solar cell conversion efficiency of 22 percent.

2.2 Results achieved

2.2.1 First tandem GaAsP on silicon solar cell was demonstrated in July 1986.

2.2.2 All four solar cell parameter goals (open-circuit voltage, short-circuit current, fill factor, and top cell transparency) required to demonstrate a 25 percent tandem solar cell have been met individually.

2.2.3 Best top solar cell results to date:

$\frac{V_{oc}}{(\text{volts})}$	$\frac{J_{sc}}{(\text{mA/cm}^2)}$	$\frac{FF}{}$	$\frac{Eff.}{(\%)}$
0.901	19.8	0.8	10.6

2.2.4 Jsc vs Eg results for the range of GaAsP compositions are 60 to 80 percent quantum efficiency for the entire range.

2.2.5 MIS and p-n junction solar cells were compared.

2.2.6 Morphology improvements were demonstrated by supersaturated melts.

2.2.7 Active layer dislocation level were reduced by multilayer grading, minimizing lattice mismatch, and by bismuth grading and/or growth-interrupts.

2.2.8 Both solid-state and vapor diffusion procedures were developed.

2.2.9 Began window layer development to reduce surface recombination.

2.2.10 Device area was increased from 0.1 to 1.0 to 4.0 sq. cm.

2.2.11 A 35 percent 3-stack six-terminal tandem cell with GaAsP/GaAs (or InP)/GaInAsP has been conceived.

2.2.12 Observed shift in GaP bandedge with nitrogen doping, and attempted to increase photon absorption in indirect GaP material.

3. CONCLUSIONS

This cost effective program led to the first real tandem solar cell that was better than state-of-the-art single-junction silicon solar cells.

Twenty-two percent mechanically-stacked, four-terminal GaAsP on silicon tandem solar cells are possible with the technology developed during this program.

Mechanically-stacked, two-terminal GaAsP on silicon tandem solar cells may be prepared with this technology.

GaAsP top solar cells with an efficiency of 10.6 percent have been prepared using this technology.

Four sq.cm. prototype GaAsP top solar cells have been demonstrated.

Growth and fabrication processes for the GaAsP top solar cells are compatible with conventional semiconductor processing technology. This will enable this technology to be transferred into production with a minimum of cost and effort.

Lattice-mismatched cap layers (e.g., GaP on the top active GaAsP layer) were explored during this contract. Cap layers must be close to lattice-matched so that nucleation of the grown layer is not inhibited locally, leading to differences in junction depth in the subsequent diffusion depending on whether the dopant source is solid-phase (grown-layer) or liquid-phase (melt). Stress/strain from cap layer lattice mismatch must be isolated from the thin emitter layer and junction. These two basic problems have led to the recommendation that future work should be done on lattice-matched cap layers.

4. PERSPECTIVE AND RECOMMENDATIONS FOR FUTURE WORK

In the optimum tandem solar cell design, the top solar cell generates over two-thirds of the total tandem solar cell power. There are two viable technical approaches for the top solar cell for the mechanically-stacked tandem solar cell: GaAsP/GaP and AlGaAs/AlGaAs. Both top solar cell approaches have demonstrated good device properties. No other has made acceptable devices.

The principal advantage of GaAsP/GaP is in its rugged, transparent mechanical substrate (GaP); the disadvantage of GaAsP lies in the lattice mismatch between the substrate and the active GaAsP device layer. The lattice mismatch makes it harder to passivate the GaAsP emitter surface.

The advantage of AlGaAs is that it is lattice-matched to its substrate. Another advantage is that a range of lattice-matched AlGaAs compositions exists which makes passivation for reduced surface recombination easier. The disadvantage is that the GaAs substrates normally used for epitaxial growth of the AlGaAs are not transparent to the top solar cell subbandgap photons. This substrate must be removed by some means before assembly of the tandem device. This leads to the biggest problem: growth of a thick, mechanically-stable, transparent AlGaAs substrate.

The issue is which of these materials -- GaAsP or AlGaAs -- will result in better top solar cell performance when compared under equivalent conditions. Each material needs to be compared using fabrication techniques that optimize transparency, open-circuit voltage, short-circuit current, fill-factor, and overall conversion efficiency in a systematic way.

Present Situation:

Top Solar Cell Transparency -- This parameter affects the amount of solar photons which will reach the silicon bottom cell. It is important to the tandem cell overall conversion efficiency that the top solar cell be completely transparent to photons less energetic than the bandgap of the top cell. AstroPower has achieved greater than 95 percent transparency on GaAsP top solar cell structures during this contract and in [19].

The key to practical AlGaAs top solar cells lies in maintaining a high degree of transparency while preparing thick (approximately 100 micron thickness) AlGaAs layers. This will eliminate the problems caused by the thin, very fragile AlGaAs layers that were investigated by others [20,21]. In recent work in our laboratories, 91 percent subbandgap transmission was achieved on a self-supporting 120-micron AlGaAs structure. Minor changes in substrate carrier concentration and the design of an improved AR coating will lead to transparencies of greater than 96 percent, which meets the mechanical stack design. Furthermore, there has been a recent breakthrough in light-emitting diode efficiency, achieving an external quantum efficiency of 8.0 percent, and resulting in LED's which are over 10 times brighter than earlier devices. These LED's were prepared by liquid-phase epitaxial growth of thick free-standing AlGaAs structures [22]. This same technology of rugged, transparent self-supporting AlGaAs layers can be applied to practical top solar cells.

Open-Circuit Voltage -- Both GaAsP and AlGaAs top solar cells have been prepared in our laboratory with Voc's of 1.3 to 1.55 volts. In recent preliminary work here on AlGaAs, Voc of greater than 1.30 volts was achieved after a short period of time and effort. Further improvements in Voc may be expected from improved p/n junction uniformity and from reduced device dark current [9].

Short-Circuit Current -- The design and practical attainment of III-V solar cells with near-theoretical Jsc values have required an effective surface passivation to minimize high surface recombination velocities (S_R). With GaAs and lattice-matched AlGaAs, this has been accomplished, in state-of-the-art solar cells, by the use of a higher bandgap heteroface. The high surface recombination velocities for the non-passi-

vated GaAs surface result from "pinning" of the Fermi level and are now attributed [23] to elemental arsenic or arsenic ions at the semiconductor surface which occur as products of the reaction between the III-V surface and air. Elimination of this arsenic has considerable potential for reduction of S_R in these materials, and appears especially attractive for GaAsP devices at this time.

Surface recombination may be reduced by orders of magnitude by "unpinning" the Fermi level at the emitter surface [23]. GaAs "pinned" and "unpinned" band diagrams are shown in Figure 14. "Unpinning" is expected to result in sizeable increases in current collection and reduced dark current (leading to higher Voc) for the GaAsP top solar cells. Woodall and coworkers [24] have shown recently that arsenic in the oxide film on GaAs is responsible for high surface recombination in devices made from that material. Yablonovitch and coworkers [25] have used inorganic sulfide films on GaAs to reduce surface recombination rates to that of the nearly ideal AlGaAs/GaAs interface.

It is clear, at the present time, that surface recombination is the major limitation to J_{sc} in GaAsP p/n junction top solar cells. The Fermi-level pinning mechanism involving metallic arsenic or arsenic ions at the semiconductor surface applies to GaAsP for the same reason it applies to GaAs. Therefore, there is a well-defined need to establish a suitable surface passivation film, eliminating the arsenic, and any other Fermi pinning mechanism, for GaAsP p-n junction top solar cell devices. This will lead to nearly ideal J_{sc} values and lower dark currents in the top solar cells. Our expectations are that J_{sc} will exceed the 14.9 mA/cm^2 required for a 25 percent tandem stack with the use of inorganic sulfide passivation films on GaAsP.

Fill Factor -- Improvements in emitter surface recombination are expected to improve the fill factor as a result of reduced dark current. Fill factor will be affected by the series resistance of the substrate. The overall design of both AlGaAs and GaAsP device structures must optimize substrate series resistance, thickness (mechanical strength), and free carrier optical absorption (transparency).

Efficiency -- AstroPower has achieved top solar cell efficiencies of over 10 percent with both GaAsP and AlGaAs materials. To put this in perspective, 13.5 percent is required for 4-terminal, 2-junction efficiency of 25 percent with state-of-the-art silicon bottom solar cells. As a result of the GaAsP program, we have prepared GaAsP solar cells with overall efficiencies of 10.6 percent (AMO). In addition to this, we have recently made lattice-matched AlGaAs top solar cells with 11.2 percent overall conversion efficiency. These results,

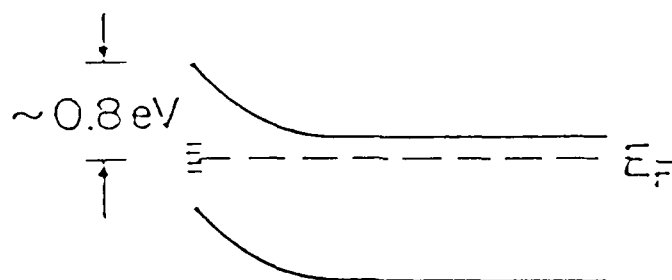


Figure 14A. "Pinned GaAs Band Structure.

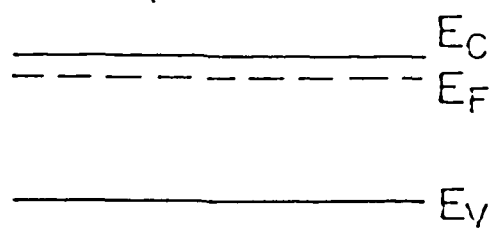


Figure 14B. "Unpinned" GaAs Band Structure.

combined with the greater than 90 percent subbandgap transparency for AlGaAs, are very encouraging.

The present day technology for "unpinning" the Fermi level, as a means of surface passivation, is in its early stages of development. Unpinning effects currently are transient and short term laboratory demonstrations. The current technology is sufficient for a fair comparison of the relative GaAsP and AlGaAs performance potential. Then, if GaAsP is determined to be the material of choice, the problem is quite clear for GaAsP top solar cell development:

- o Develop the growth and fabrication of a nearly lattice-matched window layer that meets the requirements indicated in 2.1.3.4 of this report; or
- o Develop a long-term, space-qualified surface "unpinning" passivation treatment.

With improved S_R for GaAsP and thick self-supporting AlGaAs, a meaningful comparison of the two top solar cell technologies can be made with immediate benefits for the Air Force in terms of overall conversion efficiency, array size, survivability, and manufacturability.

In summary, the present opportunity for comparing AlGaAs and GaAsP top solar cell technologies on a quantitative basis in the same laboratory is very attractive. Our recommendations for taking advantage of this opportunity will compare self-supporting (approximately 100 microns thick) AlGaAs top solar cells and surface-passivated GaAsP (on transparent GaP) top solar cells. This work is expected to establish which top solar cell material will exhibit the most promise for 25 percent to 35 percent tandem solar cells.

REFERENCES

- [1] H.B. Curtis, C. K. Swartz, R. E. Hart, "Radiation Performance of AlGaAs and InGaAs Concentrator Cells and Expected Performance of Cascade Structures," 19th IEEE Photovoltaic Specialists Conference, New Orleans, p. 727, (1987).
- [2] H.C. Hamaker, J. G. Werthen, C. R. Lewis, H.F. MacMillan, C.W. Ford, G.F. Virshup, R.K. Ahrenkeil, D. L. Greenberg, J. Schlupmann, "Radiation Damage of 1.93-eV $Al_{0.37}Ga_{0.63}As$ and GaAs Solar Cells Grown by Metalorganic Chemical Vapor Deposition," 19th IEEE Photovoltaic Specialists Conference, New Orleans, p. 733, (1987).
- [3] Personal communication, Dr. Robert Walko, Sandia National Laboratories.
- [4] M. Wolf, "A New Look at Silicon Solar Cell Performance," Energy Conversion, 11, 63 (1971).
- [5] M.E. Nell and A.M. Barnett, "The Spectral p-n Junction Model

- for Tandem Solar Cell Design," IEEE Transactions on Electron Devices, ED-34, 257-266, (1987).
- [6] N. E. Terranova and A. M. Barnett, to be published.
 - [7] R.A. Sinton, Y. Kwark, J.Y. Gan, and R.M. Swanson, "27.5% Silicon Concentrator Solar Cells," IEEE Electron Device Letters, EDL-7, (#10), 567-569, 1986.
 - [8] M.A. Green, Z. Jianhua, A.W. Blakers, M. Taouk, and S. Narayanan, "25-Percent Efficient Low-Resistivity Silicon Concentrator Solar Cells," IEEE Electron Device Letters, EDL-7, (#10), 583-585, 1986.
 - [9] A.M. Barnett and J.S. Culik, "New Solar Cell Design Options," 19th IEEE Photovoltaic Specialists Conference, 931, New Orleans, (1987).
 - [10] M. Gillanders, B. Cavicchi, D. Lillington, N. Mardesich, "Pilot Production Experience of LPE GaAs Solar Cells," 19th Photovoltaic Specialists Conference, 289, New Orleans, (1987).
 - [11] H. Nelson, "Depositing Successive Epitaxial Layers from the Liquid Phase," U.S. Patent 3,565, 702 issued February 23, 1971.
 - [12] J. M. Woodall, H. J. Hovel, "An Isothermal Etchback-Regrowth Method for High-Efficiency $Ga_{1-x}Al_xAs$ -GaAs Solar Cells," Appl. Phys. Lett., 30(9), 492, 1977.
 - [13] M. W. Wanlass, K. A. Emery, M. M. Al-Jassim, A.R. Mason, "Effect of Defect Density and Compositional Grading on GaAsP Photovoltaic Performance," Conf. Rec. 19th IEEE Photovoltaic Specialists Conference, 530, New Orleans, (1987).
 - [14] S. C. Chang, G. Y. Meng, D. A. Stevenson, "In Situ Electrochemical Monitoring and Control of Oxygen in Liquid Phase Epitaxial Growth of GaAs," J. Crystal Growth, 62, 465-474 (1983).
 - [15] H.J. Hovel, J.M. Woodall, "Improved GaAs Solar Cells with Very Thin Junctions," Conf. Rec. 12th IEEE Photovoltaic Specialists Conference, p.945, New York 1976.
 - [16] B.Schwartz, "GaAs Surface Chemistry - A Review" CRC Critical Reviews in Solid State Sciences, p. 609-624, November 1975.
 - [17] R. Z. Bachrach, "Optical Techniques Useful for Characterizing GaP Crystals," J. Electronic Materials, 3(3), 645, 1974.
 - [18] D. J. Olego, R. Schachter, J. A. Bauman, "Passivation of the GaAs Surface by an Amorphous Phosphorus Overlayer," Appl. Phys. Lett., 45(10), 1127 (1984).
 - [19] G.H. Negley, J.B. McNeely, P.G. Lasswell, E.A. Gartley, A.M. Barnett, T.M. Trumble, "Design and Development of GaAsP on GaP/Silicon Mechanically Stacked, Multijunction Solar Cells," 19th IEEE Photovoltaic Specialists Conference, 119, New Orleans (1987).
 - [20] R. J. Boettcher, P. G. Borden, M. J. Ludowise, "Ultrathin GaAs and AlGaAs Solar Cells," 16th IEEE Photovoltaic Specialists Conference, 1470, San Diego, (1982).

Also Sandia Contract SAND68-2264 Final Report.

- [21] S. W. Zehr, J. A. Cape, D. L. Miller, H. T. Yang, "Status of Rockwell-ERC High Efficiency Solar Cell Programs," Space Photovoltaic Research and Technology 1980, NASA CP-2169, 113, (1980).
- [22] H. Ishiguro, K. Sawa, S. Nagao, H. Yamanaka, S. Koike, "High Efficiency GaAlAs Light-Emitting Diodes of 660 nm with a Double Heterostructure on a GaAlAs Substrate," Applied Physics Letters, 43(11), 1034, (1983).
- [23] A.L. Robinson, "Chemical Coat Helps Semiconductor Prospects," Science, 238, 27, (1987).
- [24] S.D. Offsey, J.M. Woodall, A.C. Warren, P.D. Kirchner, T.I. Chappell, G.D. Pettit, "Unpinned (100) GaAs Surfaces in Air Using Photochemistry," Applied Physics Letters, 48(7), 475, (1986).
- P.D. Kirchner, A.C. Warren, J.M. Woodall, C.W. Wilmsen, S. L. Wright, J. M. Baker, "Oxide Passivation of Photochemically Unpinned GaAs," J. Electrochem. Soc., to be published.
- [25] E. Yablonovitch, C.J. Sandroff, R. Blat, T. Gmitter, "Nearly Ideal Electronic Properties of Sulfide Coated GaAs Surfaces," Applied Physics Letters, 51(6), 439, (1987).